National Library of Canada
Acquisitions and Bibliographic Services Branch
395 Wellington Street
Ottawa, Ontario
K1A 0N4

Bibliothèque nationale du Canada
Direction des acquisitions et des services bibliographiques
395, rue Wellington
Ottawa (Ontario)
K1A 0N4

Your file Votre référence

Our file Notre référence

NOTICE

The quality of this microform is heavily dependent upon the quality of the original thesis submitted for microfilming. Every effort has been made to ensure the highest quality of reproduction possible.

If pages are missing, contact the university which granted the degree.

Some pages may have indistinct print especially if the original pages were typed with a poor typewriter ribbon or if the university sent us an inferior photocopy.

Reproduction in full or in part of this microform is governed by the Canadian Copyright Act, R.S.C. 1970, c. C-30, and subsequent amendments.

AVIS

La qualité de cette microforme dépend grandement de la qualité de la thèse soumise au microfilmage. Nous avons tout fait pour assurer une qualité supérieure de reproduction.

S'il manque des pages, veuillez communiquer avec l'université qui a conféré le grade.

La qualité d'impression de certaines pages peut laisser à désirer, surtout si les pages originales ont été dactylographiées à l'aide d'un ruban usé ou si l'université nous a fait parvenir une photocopie de qualité inférieure.

La reproduction, même partielle, de cette microforme est soumise à la Loi canadienne sur le droit d'auteur, SRC 1970, c. C-30, et ses amendements subséquents.

Canada

UNIVERSITY OF ALBERTA

Survey and Applications of Contact Sensing

by

© **Raju Patil**

A thesis
submitted to the Faculty of Graduate Studies and Research
in partial fulfillment of the requirements for the degree
of **Master of Science**

Department of Computing Science

Edmonton, Alberta
Spring 1994

National Library
of Canada

Acquisitions and
Bibliographic Services Branch

395 Wellington Street
Ottawa, Ontario
K1A 0N4

Bibliothèque nationale
du Canada

Direction des acquisitions et
des services bibliographiques

395, rue Wellington
Ottawa (Ontario)
K1A 0N4

Your file Votre référence

Our file Notre référence

The author has granted an irrevocable non-exclusive licence allowing the National Library of Canada to reproduce, loan, distribute or sell copies of his/her thesis by any means and in any form or format, making this thesis available to interested persons.

L'auteur a accordé une licence irrévocable et non exclusive permettant à la Bibliothèque nationale du Canada de reproduire, prêter, distribuer ou vendre des copies de sa thèse de quelque manière et sous quelque forme que ce soit pour mettre des exemplaires de cette thèse à la disposition des personnes intéressées.

The author retains ownership of the copyright in his/her thesis. Neither the thesis nor substantial extracts from it may be printed or otherwise reproduced without his/her permission.

L'auteur conserve la propriété du droit d'auteur qui protège sa thèse. Ni la thèse ni des extraits substantiels de celle-ci ne doivent être imprimés ou autrement reproduits sans son autorisation.

ISBN 0-612-11321-3

Canada

UNIVERSITY OF ALBERTA

RELEASE FORM

NAME OF AUTHOR: **Raju Patil**

TITLE OF THESIS: **Survey and Applications of Contact Sensing**

DEGREE: **Master of Science**

YEAR THIS DEGREE GRANTED: **1994**

Permission is hereby granted to the UNIVERSITY OF ALBERTA LIBRARY to reproduce single copies of this thesis and to lend or sell such copies for private, scholarly or scientific research purposes only.

The author reserves all other publication rights and other rights in association with the copyright in the thesis, and except as hereinbefore provided neither the thesis not any substantial portion thereof may be printed or otherwise reproduced in any material form whatever without the author's prior written permission.

(Signed) Rajpatil . . . . . .

Permanent Address:
Sumati Niwas,
Deenbandhu Colony,
Karwar Road,
Hubli, Karnataka
India – 580 029

Date: 21 Dec '93

UNIVERSITY OF ALBERTA

FACULTY OF GRADUATE STUDIES AND RESEARCH

The undersigned certify that they have read, and recommend to the Faculty of Graduate Studies and Research for acceptance, a thesis entitled **Survey and Applications of Contact Sensing** submitted by **Raju Patil** in partial fulfillment of the requirements for the degree of **Master of Science**.

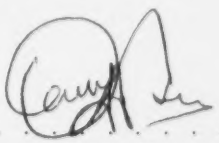

Dr. A. Basu (Supervisor)

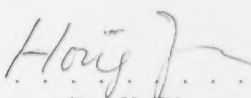

Dr. H. Zhang

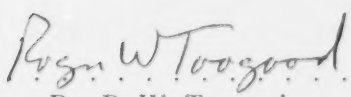

Dr. R. W. Toogood

Date: 20 Dec '93

To my family

Abstract

The emphasis in robotics research is shifting from the design of highly dextrous manipulators to the design of "intelligent" robots, leading to an increased use of sensors in robots. Recent research in sensory systems for robotic applications has prompted an interest in the study of the human sensory system, which till now has always been studied from a medical or psychological point of view. Of the five human senses, the important ones from a robotics perspective are the senses of vision and touch. Vision cannot be employed in many situations, especially in areas of low visibility. We consider the possibility of employing "contact sensing" in such situations. In this thesis, we discuss human and robotic contact sensing and consider the use of contact sensing to detect the presence of cracks in surfaces.

Detecting cracks in surfaces is a problem with many practical applications. The manual inspection of ship hulls is a difficult and time consuming process. Another example is the inspection of underground pipes for surface cracks. An automated inspection system which can perform inspection of surfaces and report the presence of cracks will therefore be of great benefit. We describe a robotic system which utilizes force sensing to *feel* surfaces and detect the presence of cracks.

Acknowledgments

I would like to thank Anup Basu, my supervisor, and Hong Zhang for their constant encouragement and support. They were a source of continuous guidance and ensured that I stayed focused on my research.

Thanks are also due to Roger Toogood for his patience and time in reading my thesis.

I would like to thank Pavan Sikka for all the timely and patient help during my experiments. I would also like to thank Steve Sutphen for fabricating the sensor module used in my experiments and for his constant hardware assistance. Thanks are due to Narendra Ravi for his help in fine tuning my document preparation and to my friends who were great company during these two years in Edmonton.

I would not have achieved what I did without the love and support of my uncle, parents and brother.

Contents

1 Introduction 1

2 Human Tactile Sensing 4

2.1 Sensation and Perception 5

2.1.1 Classical Threshold Theory 6

2.1.2 Quantitative Study of Stimulus Perception 7

2.2 The Nervous System 10

2.2.1 Signal Transmission in Neurons 12

2.3 Tactile Receptors 13

2.3.1 Proprioceptive Sensor System 13

2.3.2 Exterioceptive Sensor System 13

2.4 Contact Sensing Functions of the Hand 15

2.5 Conclusion 16

3 Robotic Tactile and Force Sensing 17

3.1 Sensors and Transducers 18

3.1.1 Sensor Classification 19

3.1.2 Performance Characteristics 20

3.2 Robotic Contact Sensing 21

3.2.1 Touch Sensor Arrays 24

3.2.2 Compliant Tactile Sensors 28

3.2.3 Additional Touch Sensors 28

3.3 Force and Torque Sensors 29
3.3.1 Joint Torque Sensing 29
3.3.2 Load Cell Structures 30
3.3.3 Strain Gauge Structures 30
3.3.4 Wrist Force Sensor 31
3.4 Sensor Data Fusion 31
3.5 Conclusion 32

4 Crack Detection by Contact Sensing **33**
4.1 System Description 35
4.2 Modeling of a Linear Potentiometer 37
4.3 Model Including the Force Sensor 42
4.3.1 System Parameter Estimation 45
4.4 Experimental Results 50
4.4.1 The Vertical Force Response 51
4.4.2 Noise 52
4.4.3 The Torque about the Sensor's Y-axis 59

5 Conclusion **61**

Bibliography **63**

List of Figures

2.1 The general structure of a neuron. 10

2.2 Nerve supply to the fingerprint skin of the hand [22]. 14

3.1 Digital tactile sensor. 26

4.1 Schematic diagram of the robot with sensors. 35

4.2 The photograph of the robot with wrist mounted sensors. 36

4.3 A closeup of the wrist with the sensors. 37

4.4 Spring-Damper model. 38

4.5 Spring extension into a crack. 39

4.6 Step response of the spring. 41

4.7 System model. 41

4.8 Simplified system model. 44

4.9 Oldenbourg-Sartorius method. 46

4.10 Smith's method: Damping ratio Vs Time ratio. 47

4.11 Smith's method: Natural frequency Vs Time ratio. 48

4.12 Smoothed step response data. 49

4.13 Actual data and the model's approximation 50

4.14 The coordinate frame assignment of the force-torque sensor. . . . 51

4.15 A typical vertical force signal. 52

4.16 The force signal when the robot is stationary. 52

4.17 The force signal when the robot is moving without touching any surface. 53

4.18 The force signal when the robot is moving with its tip in contact with a flat surface. 54

4.19 The effect of wheel diameter on the input to the sensor. 55

4.20 The effect of wheel diameter on the force response when the width of the crack is less than the wheel diameters. 56

4.21 There is no effect of wheel diameter on the force sensor when the width is larger than the wheel diameters. 57

4.22 The vertical force response is higher for wider cracks. 58

4.23 The force and torque signals for a crack of width 7 mm and depth 0.5 mm. 59

4.24 The force and torque signals for a crack of width 2 mm and depth 1 mm. 60

4.25 The force and torque signals for a crack of width 20 mm and depth 3 mm. 60

Chapter 1

Introduction

The development of highly dextrous manipulators has been a major concern of robotics researchers for a long time. The major emphasis has been on issues such as accuracy, repeatability and payload. Highly efficient manipulators have been designed which are capable of executing specific kinds of tasks in controlled environments. Since the design and development of these robots has been motivated by industrial needs, the branch of robotics dealing with such robots is classified as "industrial robotics". However, industrial robots are able to work only in environments which are static and enough knowledge of which is known to the robot. Therefore, industrial robots are limited in their effectiveness. More often than not, robots are required to work in changing environments or in certain hazardous areas, enough information of which is not available beforehand. Recent research in robotics has tried to address the problem of automation in unstructured environments. Researchers are attempting to equip robots with "intelligence", resulting in the growth of a new branch of robotics called "intelligent robotics". A part of this drive towards more intelligent robotics is fueled from advances in artificial intelligence. The developments in areas such as knowledge based reasoning and self-learning systems have had direct applications in robotics.

In order to "learn" about their environment, and execute tasks in unstructured

environments, or environments which change with time, robots need to gather external information. This information can be obtained by means of various sensors. Visual, tactile, position, and various other kinds of information can be provided by different kinds of sensors. Even in highly structured environments, certain tasks can be accomplished only with the help of sensing mechanisms. An example of this kind of task is that of fine manipulation of small parts. A task such as insertion of a small part into a hole can be accomplished by making use of force sensors mounted in the end effector of the robotic manipulator. Modern robotic systems are feedback control systems, typically consisting of a manipulator equipped with multiple sensors. These sensors provide information about the outside world to the robot, and this information is used by the robot to assist it in the performance of user desired tasks.

Research in sensory systems for robotic applications has prompted an interest in the study of the human sensory system, which until now has always been studied from a medical or psychological point of view. The human sensory system is very complex and remains incompletely understood to date. Of the five human senses, the important ones from a robotics perspective are the senses of vision and touch. Robots are increasingly equipped with cameras and force and touch sensors, and computer vision and tactile/force sensing are actively researched fields.

In this thesis, we concentrate on tactile and force sensing, which are together referred to as contact sensing. In many applications, contact sensing plays an important role in conjunction with vision. For example, in certain applications involving fine manipulation, visual feedback is used for gross positioning and contact sensing is used for fine control. In certain applications involving low visibility areas, vision cannot be used at all, and contact sensing is the only source of external information. We consider one such application in this thesis. The problem is that of detecting cracks in the surfaces of objects which are underwater or in

sludge filled areas, where vision cannot be employed. We attempt to obtain the required information by means of contact sensing, specifically force sensing.

The organization of the thesis is as follows: Chapter 2 is a survey of human contact sensing, with special emphasis on the physics of touch. Chapter 3 is a survey of robotic contact sensing, with a discussion of performance characteristics of sensors. Chapter 4 discusses the problem of detection of cracks in object surfaces, and presents the details of the system used to perform the task. Chapter 5 suggests areas of future work.

Chapter 2

Human Tactile Sensing

Human beings are able to perform complex manipulation tasks and are able to deal with a dynamic and unpredictable environment. This ability is due, in no small measure, to the highly developed sensory system of human beings. Many researchers attempting to equip robots with sensing abilities have sought to understand the human sensory system and draw from this knowledge to develop robotic sensors. We will discuss the human tactile sensing mechanism in this chapter.

Human tactile sensing is a complex mechanism. The human body is covered all over with a sensitive skin. Sensory information about the position and type of contact with an object is provided by the sensors in the skin. The nerve endings in the surrounding muscles and tendons provide position and force information. Reflex control is provided by the spinal cord. The higher levels in the nervous system, the cerebellum, subcortex and cerebral cortex, provide more sophisticated control. The cerebral cortex coordinates lengthy tasks making use of other sensory information. Visual information is a major information contributor to the cerebral cortex [3].

The sensitivity of the skin varies with its location on the body, but the general sensory mechanism remains the same. This chapter discusses the sensory mechanism of the skin. Section 2.1 discusses the physiological and psychological aspects

of sensation and perception. Section 2.2 presents a brief outline of the human nervous system. Section 2.3 discusses the classification of the sensory systems which react to contact with external objects and presents the details of each type. Section 2.4 discusses the tactile functions of the hand.

2.1 Sensation and Perception

A distinction is normally made between the terms sensation and perception. Sensations are simple experiences brought about by simple stimuli whereas perceptions are more complicated experiences brought about by complex stimuli [10]. Examples of sensation in the above sense are the sensation of "light" on seeing a bright flash of light and the sensation of "pain" on being pinched etc. Thus, sensation refers to some simple activity of any of the sensory receptors. Perception involves a more complicated mechanism, and is accomplished by a combination of simpler sensations. The process of perception involves memory and may be affected by a person's past experience. Perception is therefore linked to a complex set of activities, necessarily involving the brain.

However, it is difficult to make the above distinction between sensation and perception. As pointed out in [10], it is difficult to draw a line between simple things (sensation) and complex ones (perception). For instance, the reaction to a simple stimulus such as a pin prick might depend on the person's cultural background, his/her personal disposition, and on the relationship of the person delivering the pin prick to the subject. A bellicose person might take umbrage at the slightest of irritations, while a mild mannered person will be calmer. Similarly, the reaction to a friendly irritant is milder compared to a hostile one.

We shall use the term sensation to refer to the low level processes occurring solely in the sensory receptors, such as the chemical changes occurring in the sen-

sory nerve endings, or electrical activity in some sensory receptors. The collection of information of such physical/chemical/electrical processes and their interpretation by the central nervous system, more specifically the brain, will be considered as perception. This chapter will mainly concentrate on "sensation" of the tactile kind in the human body and will only briefly discuss "tactile perception".

2.1.1 Classical Threshold Theory

We shall now consider some quantitative aspects of sensation which will be useful in modeling human tactile sensing. It is known that a certain minimum stimulus is necessary to excite the sensory nerves. The smallest amount of stimulus energy necessary for an observer to detect the stimulus is termed as "absolute threshold" [10]. J. F. Herbart first proposed the concept of an absolute threshold in the early 1800's, and Gustav Fechner [8] and others after him, developed this concept into the **classical threshold theory**. According to this theory, there is a sharp transition between a state in which an observer cannot detect the stimulus (when the stimulus intensity is below the threshold) and in which the observer can detect the stimulus (when the stimulus intensity is above the threshold) [10]. The explanation for this threshold is that there is some level of nerve activity always, called spontaneous activity, even in the absence of stimulation. Therefore, a stimulus would be detected only when it causes some critical increase in neural activity above the spontaneous level [10], just as a voice would be heard only when it is sufficiently louder than the noise level in a room full of people conversing with each other. Though this theory is at a "perceptual" level, it can be applied at the "sensation" level as well.

Actual measurements however, show a gradual transition between not detecting the stimulus and detecting it. Classical threshold theory explains this difference as occurring due to the fact that the various factors, such as the level of

spontaneous activity in the nerves, and the sensitivity of the receptors etc. do not remain constant during the experiment. Therefore, different threshold levels exist at different points in time.

In 1928, Adrian [1] propounded the "all-or-nothing-law", according to which the responses of a neuron to a stimulus were thought to be of two kinds only: either the neuron exhibited some response or did not; there is no gradation of responses based on differing strengths of inputs. He attributed this to the fact that the stimulus merely triggered the impulse and did not contribute to the energy needed for its transmission. Later studies of electrical changes within the nerve cell and its dendrites established that the "all-or-nothing" law applies only to the axon of the nerve cell, and that the central nervous system exhibits a graduated response. The graduated response of the central nervous system is due to the fact that the impulses in one fiber add to the impulses in another and these two impulses form a summing input to a secondary neuron. Depending on the input, either of the following can occur: (1) Only one of the input fibers may fire in which case the secondary neuron does not fire (2) Both input fibers may fire in which case the secondary neuron also fires. This phenomenon has been observed in the spinal cord, thalamus and the cortex.

2.1.2 Quantitative Study of Stimulus Perception

We will digress for a short while (from sensation to perception) and discuss a couple of laws which attempt to model the way our brain perceives stimuli which are above the threshold value. We will consider the relation between the intensity of applied stimulus and our perception of its magnitude. It can be observed that the perceived strength of a stimulus is not linearly related to its actual strength. If the intensity of sound is doubled, the listener does not feel the sound as twice as loud. Similarly, light from some source will not look twice as bright even

if its intensity is doubled. Fechner and Stevens have proposed two approaches to measure the relationship between the intensity of applied stimulus and its perceived magnitude.

Fechner's Law

Gustav Fechner based his relation on *Weber's law*. E. H. Weber in 1834 conducted experiments [10] in which observers were asked to determine the heavier weight among a standard weight and a comparison weight by lifting each weight in turn. By repeated experiments with different weights, he determined the *difference threshold*, the smallest difference between two weights that could be reliably differentiated. The size of the difference threshold, also called *just noticeable difference* (*JND*), depends on the weight of the stimulus. The *JND* gets larger as the stimulus gets larger. Weber determined the size of the *JND* to be a constant fraction of the size of the stimulus, expressed mathematically as follows (Weber's law):

$$JND = KS \tag{2.1}$$

where K is a constant called *Weber's fraction*, and S is the value of the standard stimulus.

Fechner based his derivations on the assumptions that Weber's law was valid and that the *JND* is the basic unit of perceived magnitude (i.e., one *JND* is perceptually equal to another *JND*) [10]. According to Fechner, the perceived magnitude P is related to the stimulus intensity I as follows:

$$P = K log I \tag{2.2}$$

Fechner's relation is based on the assumption that Weber's law is correct, but Weber's law is not valid when stimulus values are close to the threshold values. Also, Weber's law is based on the assumption that the *JND* is the basic unit of

measurement and that an intensity that is $2N$ *JNDs* above threshold should result in the perceived magnitude being twice as large as an intensity N *JNDs* above threshold. But S. Stevens in 1936 showed that a sound $2N$ *JNDs* above threshold sounds much more than twice as loud as a sound N *JNDs* above threshold and later (in 1957) published a paper [28] strongly criticizing Fechner's law (which till then had only been tentatively questioned by a few researchers but never seriously challenged). Stevens proposed a law which better explained the relation between the intensity of a stimulus and its perceived magnitude than Fechner's law.

Stevens' Power Law

Stevens' developed a method called *magnitude estimation*. A standard stimulus is presented to the observer and is assigned a value n. Then different intensities of the stimulus are presented and the observer is asked to assign values proportional to the estimated magnitude of each of these stimuli. If the stimulus appears twice as intense as the standard one, it is assigned a value of $2n$, if it appears half as intense, it is assigned a value of $n/2$ and so on.

Stevens conducted magnitude experiments for brightness, for the length of a line, and for the sensation caused by an electric shock presented to the finger. The plots of estimated magnitudes against stimulus magnitudes are given in [29]. The curve for brightness exhibits *response compression*. Doubling the intensity of light causes less than a doubling of the perceived brightness. The curve for the shock exhibits *response expansion*. Doubling the shock results in more than double the sensation of the shock. The curve for line length is *linear*. Doubling the line length results in the observer's estimate also doubling. Stevens' power law is a common equation for all these kinds of curves and is obtained by replotting the curves on a log-log scale.

When the logarithm of the perceived magnitude is plotted against the logarithm of the stimulus intensity, all the curves become straight lines. Straight line functions on such a log-log plot are called **power functions** [10] and are described by the relation:

$$P = KI^n \tag{2.3}$$

where P is the perceived magnitude and I is the stimulus intensity. The above relation is called Stevens' power law. The exponent n indicates the slope of the lines, and is different for different kinds of stimuli.

2.2 The Nervous System

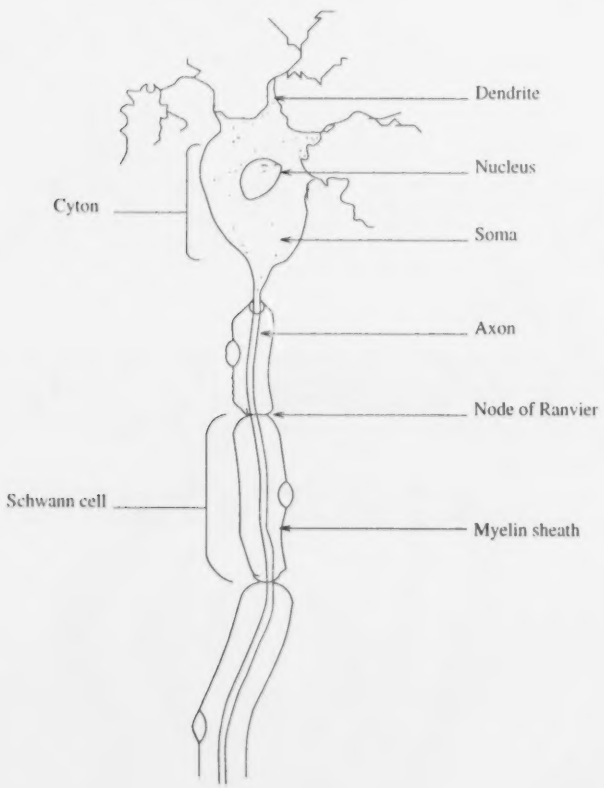

Figure 2.1: The general structure of a neuron.

The nervous system is a communication system that transforms environmental energy into electrical energy and then transmits this electrical energy from one part of the body to another [10]. The term environmental energy encompasses light energy, mechanical energy and chemical energy. All these forms of energy must be transformed to electrical impulses to be understood by the brain. This transformation of energy is performed by the *sensory receptors*. The receptors for each sense (sight, smell, touch, hearing, taste) are specialized to respond to a specific type of energy. The details of touch receptors are mentioned later in the section on tactile receptors. Once the transformation of energy is done by the sensory receptors, the electrical signals generated have to be transmitted to the brain. This is done by the cells called *neurons*. Various nerve cells appear very diverse in structure, but they have many common features. Each neuron consists of a cell body, called *cyton* which receives the electrical signals and a nerve fiber, called *axon* which transmits these signals [4] (Figure 2.1).

The cytoplasm of the cyton is called *soma*. The extensions of the cyton, called *dendrites* are specialized for the reception of signals from other neurons. The axon is responsible for transmission of the nerve impulses. The axon is covered by myelin sheath which forms cells called *Schwann cells* separated by constrictions called *Nodes of Ranvier*. The functional connection between neurons is called *synapse*. A synapse is a highly specialized structure which almost always allows impulses to cross in only one direction. A synapse passes on only those impulses which arrive in effective temporal sequence [4].

The signals transmitted by these neurons travel up the spinal cord to a structure called the *thalamus*. The signals corresponding to the sense of touch travel to the *cortical receiving area* . The thalamus has different *nuclei* where groups of synapses occur for different senses (except smell) before passing on to the brain. The cortical receiving area for touch is at the top of the cortex in the brain called

parietal lobe. Once the information is received in the parietal lobe, perception occurs, either in the parietal lobe or somewhere else in the brain.

2.2.1 Signal Transmission in Neurons

When a nerve fiber is not transmitting any electrical signal, that is, when it is at rest, the electric potential inside the fiber is negative compared to the outside of the fiber. Using a microelectrode, it has been found [10] that at rest, the potential inside the fiber is 70 mV less than the potential outside. This -70 mV potential of the inside of the fiber with respect to its outside is called its *resting potential*. Another property of nerve fibers at rest is the presence of a large number of sodium ions (Na+) outside the fiber and a large number of potassium ions (K+) inside the fiber. The propagation of electrical signals in the nerve fibers occurs by the flow of the sodium and potassium ions across the walls of the fiber. First, sodium ions move into the fiber when a stimulus is applied, causing a rise in the potential of the inner part of the fiber compared with the outer part. Then the potassium ions flow out of the fiber causing a fall of potential. This flow of sodium and potassium ions propagates down the length of the nerve fiber. The following properties of signal transmission in neurons are given in [10]. A larger stimulus does not cause a change in the potential values. In most cases, the inner potential (with respect to the outer part) varies between -70 mV to +40 mV. A larger stimulus however results in an increased rate of nerve firing. There is however an upper limit to the rate of nerve firing (500-800 impulses per second) because each fiber requires certain time called *refractory period* to recover from conducting one impulse before being able to conduct another; about one millisecond.

2.3 Tactile Receptors

The human body has two sensory systems, proprioceptive and exterioceptive. The proprioceptive system measures internal quantities such as limb joint angles, muscle extension, muscle tension etc. The exterioceptive system reacts to contacts with external things, i.e., it reacts to the changes in temperature and deformation of the skin resulting from such contact [22].

2.3.1 Proprioceptive Sensor System

The human body has some deeply embedded sensors providing it *kinesthetic sense* which allows it to respond to movements and the state of tension in muscles, tendons and joints. These sensors provide knowledge of the position of our limbs and the forces applied by the limbs on external objects. There are four types of proprioceptive sensors. Annulospiral and 'flower spray' endings, present in muscle spindles, sense the stretching of a muscle fiber. A third group of nerve endings located in muscle tendons senses muscle tension. The fourth group of nerve endings, located in the connective tissue surrounding the joints, measures limb joint angles.

2.3.2 Exterioceptive Sensor System

The skin has two main layers: the outer layer called epidermis and the layer below it called dermis. Layers of subcutaneous tissues and fat exist below the dermis. The nerve endings of the exterioceptive sensor system are located in the dermal and epidermal layers of the skin. Various specialized nerve endings are present for sensing contact pressure, texture, temperature and pain. Figure 2.2 shows the major exterioceptive sensors.

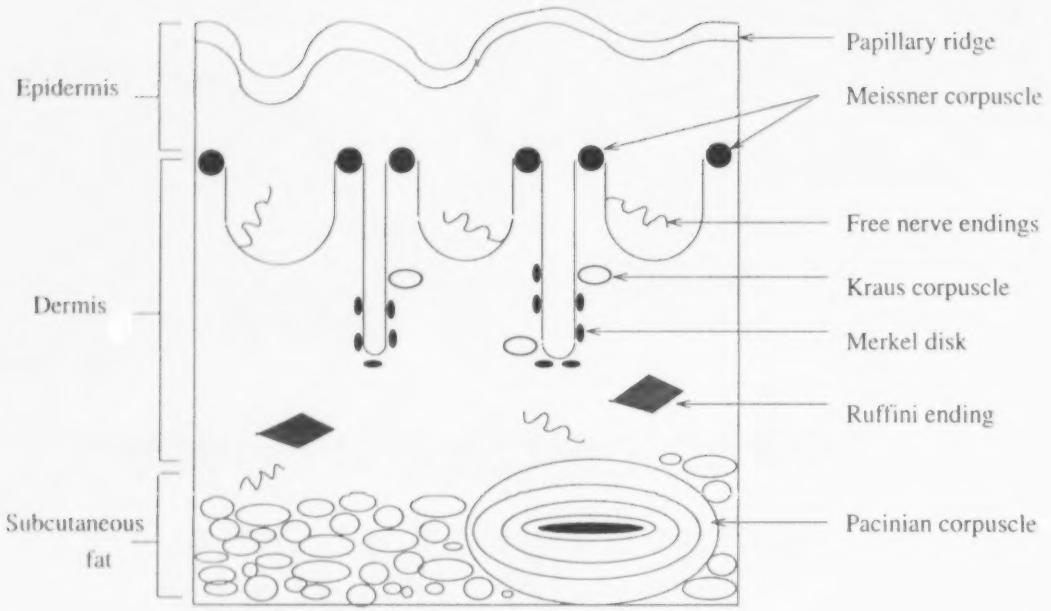

Figure 2.2: Nerve supply to the fingerprint skin of the hand [22]. (modified)

Meissner and Merkel endings are high resolution sensors close to the skin surface. Krause end bulbs (also called Krause corpuscles) are located only in specific areas of the skin such as in the eye, tongue and genital areas. Pacinian corpuscles and Ruffini endings have broader receptive fields and lie deeper inside the skin. The free nerve endings have high threshold and are sensitive to painful stimuli. Many free nerve endings may be associated with a single fiber. In addition to the receptors mentioned above, many different kinds of sensory receptors with slightly differing shapes and sizes have been identified [9]. The membrane surrounding the nerve ending determines which type of stimulus activates a particular nerve fiber. Bare nerves have a higher threshold, endings with expanded tips have a lower threshold and higher spatial resolution and so on. The manner in which the nerve endings are connected to the surrounding tissue structure also affects the response of the sensors [22].

In addition to all these sensory receptors, hairs also serve as short range prox-

imity sensors (the other function of hairs is to retain body heat). Hairs are very sensitive to touch. Russell [22] describes them as acting as levers in which slight changes in position are detected and signaled by a network of nerve endings surrounding the hair follicle.

2.4 Contact Sensing Functions of the Hand

The hand performs many functions, the most important of which are the sensory functions of touch and the function of prehension (grasping). The hand is viewed as an organ of "touch" rather than a "tactile" organ. The distinction between tact and touch is drawn in [30]. Tact is passive, touch is active and voluntary. The skin of the rest of the body undergoes passive contact but the skin of the hand is involved in active touch. The hand can act voluntarily and change its orientation with respect to an object to gain more information concerning an object. The hand goes through the stages of contact, digital touch (touching using fingers) and manual palpation (to palpate is to examine by touch) to give us knowledge or "gnosis" of an object. The recognition of the geometrical surfaces of an object is termed "stereognosis" (*stereos* in Greek means "solid"). In present usage, stereognosis is used to describe the recognition of any object by touch.

The human skin is capable of pattern recognition. Experiments have been performed by applying letter patterns to the fingertip. It has been suggested that touch works very much like blurred vision. This function of pattern recognition and other higher level functions of course occur at the perceptual level, with the involvement of the complete cutaneous nervous system (including the brain). The ability of the skin to perceive roughness of surfaces and to discriminate texture has also been established by numerous psycho-physical studies. Lederman and Browse list many references in [14] which contain details of such studies. Some

work has also been done to explain the integration of information from multiple fingers in understanding external objects.

2.5 Conclusion

We have seen the basic features of the tactile sensory system and its functions in the human body. The way the system works is not yet fully understood. Much of the work in understanding the skin's features and functions has been prompted by medical and psychological considerations. Recent research in sensory systems for robotic applications has also generated interest in the study of the human senses. As robotics moves from industrial robots working in highly structured environments to intelligent sensor equipped robots working in unstructured and/or hazardous environments, it will be necessary to develop highly efficient sensory mechanisms for the robots. A complete understanding of the human body's highly complex sensory system will be useful in this effort.

The problem studied in this thesis is that of detecting cracks in the surfaces of objects. If a human being slides her/his finger across a surface, it is easy to distinguish different irregularities in the surface. This is possible due to the extremely high resolution and sensitivity of the touch sensors in the finger and the finger's high compliance. Robotic tactile sensing suffers from low force resolution and low signal to noise ratio due to mechanical cross talk. An additional problem is the difficulty of maintaining stable planar contact with arbitrary surface contours. We therefore use force sensing to accomplish the task of crack detection.

Chapter 3

Robotic Tactile and Force Sensing

Robotics research is increasingly focused on incorporating *sensing* in robots along with the development of highly dextrous manipulators. This will enable robots to perform tasks in highly unstructured environments. At present, the majority of robots utilized are industrial robots with little or no sensory capabilities. In the kind of tasks for which industrial robots are used, the main requirements are accuracy, repeatability and high payloads. Since the industrial robots work in a strictly controlled environment, they can function without sophisticated sensory mechanisms. However, for applications where the environments are very unstructured, the need for robots to gather external information becomes inevitable. Even in a highly structured environment, some tasks involving fine manipulation dictate the need for a sensitive sensor equipped dextrous manipulator.

A wide variety of sensors is used in robots to provide visual, tactile, position and other kinds of information. In this chapter, we present the issues involved in tactile and force sensing and discuss some tactile and force sensors. Section 3.1 discusses sensors and transducers in general along with their classification and performance characteristics. Section 3.2 provides a general view of robotic tactile sensing specifications for different applications and the different

effects/phenomena and the materials used for different kinds of tactile sensors. Section 3.3 discusses force and torque sensors and section 3.4 discusses sensor data fusion briefly.

3.1 Sensors and Transducers

A sensor equipped robot can be viewed as an information processing unit [22]. An information processing unit typically consists of an input unit which is a sensor or a transducer, a processing unit which interprets the data provided by the input unit, and an output unit which provides the system's response to the processed data. The input unit acquires *information* and converts the information into a form suitable to be handled by the processor. The device which converts one form of information (energy) to another form is called a transducer. The processor uses this information provided by the input transducers in conjunction with its knowledge of the task to be performed to generate command for the actuators which accordingly move the robot.

Information is something that reduces uncertainty, according to Claude Shannon. Alternatively, information is something which adds to existing knowledge. Information flow is achieved by a transfer of energy or matter. The different forms of energy, through which information can manifest itself are as follows [22]:

- Chemical: Anything dealing with the internal structure of matter, the parameters being crystal structure, concentration of a certain material etc.
- Electrical: Any electrical phenomenon such as change in potential, current, charge or resistance.
- Magnetic: The parameters of interest are field intensity, flux density, and permeability.

- Mechanical: Any external parameter of matter such as position, velocity, acceleration, force, momentum, torque etc.
- Radiant: Any of the electromagnetic waves, ranging from radio waves to gamma rays. The parameters of interest are intensity, frequency, polarization and phase.
- Thermal: The parameters of interest are temperature, temperature gradient, heat and entropy.

3.1.1 Sensor Classification

Sensors maybe classified on the basis of the type of energy involved, the various kinds of energy being mentioned above. Sensors may also be classified as *self-generating* or *modulating* depending on whether the energy from the input signal is directly converted to the output signal or an auxiliary energy source is used, respectively. The advantages of a self-generating sensor are as follows [22]:

- It has no offset, i.e., zero input produces zero output.
- It requires no additional power source, and hence suitable for low power applications.

Selenium photoelectric cells are an example of self-generating sensors. The advantages of a modulating sensor are as follows:

- Weak signals can be detected better than in a self-generating signal since the modulator can act as an amplifier.
- Various physical effects can be used for gathering information, with the sensor output always being in the electrical domain (by choosing an electrical auxiliary power source).

Sensors based on the piezoresistive effect (change in the electrical resistance of a material with a change in applied pressure) are examples of modulating sensors. The auxiliary energy source used with such sensors is an electrical source which drives current through the piezoresistive material. A change in the resistance due to change in applied pressure results in a change in current.

Sensors are also classified as *absolute* or *incremental* [22]. Absolute sensors are those in which the sensor output represents sensor input directly. A potentiometer is an example of an absolute sensor. In an incremental sensor, only the changes in the sensor input show up in the sensor output. An incremental encoder used for determining shaft rotation is an example of an incremental sensor.

3.1.2 Performance Characteristics

The various performance characteristics of sensors are as follows [22]:

Linearity A sensor is said to be linear if equal changes in the sensor input result in equal changes in the sensor output throughout its operating range. When the output of a linear sensor is plotted against its input, a straight line is obtained. Most sensors are only approximately linear, and most are so for a restricted set of input values. A piecewise linear approximation can be used for highly non-linear sensors.

Hysteresis The sensor output for a particular value of sensor input may vary depending on whether the sensor input was increasing or decreasing when the measurement was made. This phenomenon is termed hysteresis and a hysteresis curve for a sensor can be obtained by plotting its output versus the input, by varying the input from the lowest value of interest to the highest value of interest and back again to the lowest value.

Repeatability Though a sensor is expected to give the same output when an input is applied repeatedly, this isn't the case always. Repeatability is a measure of the change in the output value when the same input is applied at different times.

Resolution The smallest change in the sensor input value in order to produce a detectable change in the sensor output value is termed as resolution. A sensor may have high resolution but low repeatability and vice versa.

Sensitivity Sensitivity of a sensor is the ratio of the change in its output to a corresponding change in the input.

Noise Noise is an unavoidable problem, especially in electrical devices. The change in the sensor output value which is not due to any change in the input is termed noise.

3.2 Robotic Contact Sensing

Dario [6] proposed the term *contact sensing* to include tactile sensing and force sensing. Tactile sensing is defined as the continuous-variable sensing of forces in an array by Harmon in [11]. Nicholls and Lee [15] define tactile sensing as the measurement of parameters of a contact interaction between the sensing device and some physical stimuli (the interaction being confined to a touch sensitive region of the device's surface). Tactile sensing is an attempt to monitor and interpret the geometrical (or sometimes chemical, thermal etc.) effects of the forces that come into play when the robot contacts an external object and it almost always involves an integration of the information from multiple input points over the contact area.

Force sensing refers to the measurement of the forces and torques generated as

a result of contact between the robot and some external object. Force sensing is thus a direct, low-level activity, whereas tactile sensing is a higher-level, *perceptual activity* [6].

Tactile sensing is used in various applications. The various application domains of robotic tactile sensing are discussed by Dario [6]. He points out that though industrial robots have been highly successful in spite of limited or no sensory capabilities, many applications demand that robots be equipped with sophisticated sensors, especially tactile sensors for tasks involving fine manipulation. Tasks which require high speed and absolute position accuracy and involve highly structured environments need not be equipped with sensors. However, tasks which require delicate operations, based on sensing local geometric features and on accurate measurements of contact forces require robots equipped with sensors. In these applications, the lower speed of operation and the higher cost resulting from the processing of large amounts of tactile and force sensor data are justified. Dario [6] terms a sensor equipped robot with highly dextrous manipulators as a *craftsman robot*.

Tactile sensors range from the very simple point contact type which detect presence or absence of touch to the more complex one consisting of a two dimensional array of sensing sites providing information on various parameters of the stimulus. Some tactile sensors which can detect slip, torque, normal forces, three-dimensional shape and thermal properties have already been developed. The dimensionality of a sensor refers to the spatial orientation of the individual sensing sites and falls into three basic classes [15].

- Zero dimension: a single point of contact, as in a limit switch.
- One dimension: a set of sensing sites arranged in a line.
- Two dimensions: a set of sensing sites arranged in a regular pattern, usually

rectangular.

In order to determine user needs and requirements in several applications utilizing tactile sensing, Harmon [11] conducted a survey in 1980, and followed it up by a study in 1982. The surveys involved 55 persons of whom 47 responded, drawn from academia, industry, research and users. The salient features of the survey are as follows:

- Approximately 90% of the respondents strongly felt that tactile sensing was needed. A few respondents were however not sure how vital touch sensing would be in the near future as they pointed out that even the simple robots existing then were underutilized in the industry.

- Specifications: The following were the most required features in tactile sensors according to the respondents.

  - Skinlike Properties: The tactile sensors should be like the human skin, i.e., they should be distributed in arrays on thin, flexible substrate, and should combine compliance and durability.

  - Smart Sensors: Processing of the information should be performed at the sensor level so that only a few output signals need be sent to the central processing unit.

  - Spatial Resolution: 1-2 mm spatial resolution was thought appropriate as this is the approximate minimum separation at which the human fingertip can distinguish two points applied to the skin as separate stimuli.

  - Array Size: As the human fingertip has about 10x15 touch sensitive points, the array size of a robotic tactile sensing system can be between 5x10 and 10x20 points per fingertip.

- Sensitivity: The force sensitivity of each force sensing element should be in the range of 0.5 to 10 grams.
- Linearity and Hysteresis: Linearity was not considered as important as stability of readings since even with a non-linear sensor, inverse computations could be easily performed. Hysteresis was considered intolerable. The tactile sensors should be highly stable, monotonic and repeatable.
- Dynamic Range: A large dynamic range was considered more important than linearity. A dynamic range of 1000:1 is reasonable.
- Time Response: The touch transducer response time should be small. The response time should be about 1-10ms.

The exact requirements of a tactile sensor for a particular application will be different, the above serving as general guidelines.

- Semiconductor and piezoelectric transduction approaches to tactile sensing were seen as most promising, while resistive and conductive materials were thought of as having little future in view of the problems of hysteresis, low sensitivity, and insufficient dynamic range, and capacitive sensing was seen as too susceptible to external fields and like magnetic sensing, too materials-dependent.
- The survey also discusses economic and social aspects of the increased use of sensing mechanisms in robots which we shall not discuss here.

3.2.1 Touch Sensor Arrays

Many different technologies have been used to make touch sensor arrays, some of which are presented in this section.

Switches

A switch is one of the simplest touch sensors. It is a binary touch sensor in that it detects the presence or absence of contact. The switch may be of the normally-open type which closes upon the application of a force exceeding some threshold value, causing some current to flow. An array of miniature switches may be employed as a tactile sensing array. However, even the smallest of miniature switches are quite large making it impossible to achieve high spatial resolution. Some useful sensors have been developed based on the idea of an array of switches.

- Pneumatic Touch Sensor: A typical pneumatic touch sensor has a shallow spherical dome of thin sheet metal [22]. The dome collapses when a force exceeding a critical value is applied, and returns to the original shape after the force is removed. The theory of elastic buckling is applied to derive relationships between the deformation and applied force in terms of the geometry of the surface and mechanical parameters of the sheet metal (Young's modulus and Poisson's ratio). An array of such switches can be connected for row and column addressing. The use of a diode in series with each switch eliminates parasitic conduction paths.

- Digital Tactile Sensor Array: Since an array of mechanical switches is too large for most applications, a digital solution has been proposed [19]. The principle used is that a sheet of elastic material when pressed against a hole, protrudes inside, and the protrusion is related to applied pressure (and to the size of the hole and elastic modulus of the sheet material). The relation (for small deflections) is as follows:

$$\delta \propto \frac{pa}{E} \tag{3.1}$$

where δ is the maximum deflection of the elastic material into the hole, p is the applied pressure, a is the radius of the hole and E is the elastic modulus of the sheet material.

Consider a sheet of conductive elastic material pressed against a V-shaped notch as shown in Figure 3.1. The pressure required to force the elastomer into the notch increases as the width decreases. This effect is used in making miniature switch arrays, each switch having a different pressure threshold [22]. The switch arrays are constructed by etching a notch into the silicon dioxide protective layer of a silicon integrated circuit.

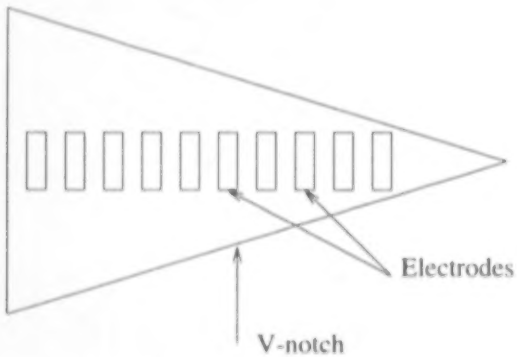

Figure 3.1: Digital tactile sensor.

Aluminum pads, each forming an electrode for a switch, are deposited along the bottom of the notch. Contact is made with each aluminum pad in turn as increasing pressure is applied. The state of the electrodes is monitored electronically to detect the applied pressure. This kind of sensor has the advantage of miniature size and direct digital output. However it is not rugged as the fragile silicon switch needs to be in contact with external objects.

Piezoresistive Touch Sensors

- Conductive Elastomers: A conducting elastomer is essentially a natural or silicone based rubber made conducting by the addition of conducting or semiconducting materials such as carbon or silver [22]. Conductive elastomers are inexpensive and easy to use. The working principle is based on the decrease in resistance when increased pressure causes a larger area of contact of the conductive elastomer with the contact pad, the two being separated by a separator mesh. Another design of sensors using conductive rubber works on the principle of changing the resistance of a piece of conductive rubber placed between two electrodes, the change being related in known way to the thickness of the rubber. As the contact force increases, the thickness of the rubber decreases, leading to a change in its resistance.

  These sensors are chemically inert and are capable of withstanding a wide range of temperatures. They can be easily molded into fingertip shape and provide a god gripping surface. However, they suffer from hysteresis, temperature dependence, creep (the sensor output changes over time for a constant load) and memory (the sensor takes time to recover to original state after the force is removed).

- Carbon Felt: A carbon felt sensor, consisting of carbon felt sandwiched between two flat electrodes, also uses piezoresistive property. With increase in pressure, the carbon fibers get compacted resulting in lower resistance and at higher pressures, the increased area of contact with the electrodes further reduces the resistance. These sensors can also be easily fabricated in desired shapes and are rugged. Sensor noise is high at low loads. These sensors suffer from a lack of compliance due to the presence of metal electrode plates.

Some tactile sensor arrays utilize piezoelectric effect. Piezoelectric effect, discovered by Jacques and Pierre Curie in 1880 is the production of electrical charge when pressure is applied to quartz crystals. Other tactile sensor arrays using optical, magnetic, photoelastic, opto-mechanical, capacitive, electrochemical and ultrasonic effects are described in [22] and [15].

3.2.2 Compliant Tactile Sensors

It is advantageous to have a compliant touch sensor because, when such a sensor is mounted on robotic fingers, a more stable grip is obtained, and the cushioning effect of compliance prevents damage to the fingers or the object. A compliant sensor has the capacity to extract three-dimensional information about the surface shape of objects. In one design of a compliant tactile sensor, a polyurethane foam is covered with an outer layer of silicone rubber which has conductive rubber strain gauges attached to the inner surface of the skin. The deformation is sensed by the strain gauges.

3.2.3 Additional Touch Sensors

The tactile sensors discussed in the previous sections determine contact forces and surface profiles of objects. Some other kinds of tactile sensors have also been developed. Proximity sensing can be performed by *whiskers* [22, 21]. Proximity sensing helps in detecting the presence or absence of objects, in searching for parts and in preventing collision damage by *feeling* the environment. The simplest type of whisker sensor is a wire passing through a small hole in a metallic plate. When the wire touches something, it gets deflected and touches the metal, thereby completing an electrical circuit. Articulated whisker probes which can orient the whisker at different angles, and thus gain information about the surface properties of objects by feeling the surface have also been developed.

Thermal sensing has received little attention so far as robots are not as sensitive to changes in temperature as human beings. However, if robots are to work in unpredictable and potentially hazardous environments, they will have to be equipped with thermal sensors. Texture sensing, slip sensing, electrical contact resistance sensing and some other sensors are discussed in [22, 15].

3.3 Force and Torque Sensors

Most of the tactile sensors discussed in the preceding sections measure force at the point of contact. This force information can be usefully employed in tasks of fine manipulation. Two other kinds of force sensing are utilized in robotics. One is the measurement of force and torque at the joints, and the other is the measurement of force and torque at the wrist.

3.3.1 Joint Torque Sensing

The motor torque is related to the armature current in a DC motor (permanent magnet or shunt wound) as follows:

$$T = K\phi I_a \tag{3.2}$$

where T is the torque developed (newton meters), ϕ is the airgap flux per pole (webers), I_a is the armature current in amperes and K is a constant for a particular motor. This relationship holds well within the operating range of a motor. While the torque so measured is useful for many purposes, factors such as friction, stiction, backlash and compliance in the drive train between the motor and robot arm joint reduce the accuracy of the information. A large amount of calculation is required to take into account the varying configuration of the robot and the effect of gravity on all the links [22].

3.3.2 Load Cell Structures

Load cell structures are regions of reduced strength in the structure of the robot, where strain is concentrated. During the normal operation of a robot, the strain is spread all over the robot body. By having an area of lesser strength, the strain can be concentrated there and so can be easily measured. However, the deliberately introduced weak point makes the robot susceptible to damage. The probability of damage is reduced by using end stops or shear pins [22]. End stops limit the deflection of the load cell elastic members to a safe value and shear pins tear off rather than transmit damaging shocks to the robot.

3.3.3 Strain Gauge Structures

The strain gauge is a transducer used for the measurement of dimensional variations within mechanical systems [20]. It is essentially a resistive or piezoresistive device, since its electrical resistance varies with pressure. A force applied to a resistive strain gauge causes a change in the physical dimension of the strain gauge, which changes the resistance. In a piezoresistive strain gauge, the resistance varies with pressure.

The sensitivity of a strain gauge is measured by a factor called *gauge factor*, G_f which is the ratio between the unit change in the electrical resistance and the unit change in the physical length.

$$G_f = \frac{\Delta R/R}{\Delta L/L} \tag{3.3}$$

Strain gauges are either metal ones (resistive) or semiconductor ones (piezoresistive). Metal strain gauges are made of a very thin metal film pattern bonded to a flexible and electrically insulating material. Semiconductor strain gauges are

fabricated as thin layers of doped silicon or germanium.

3.3.4 Wrist Force Sensor

A wrist force sensor is typically a load cell combined with strain gauges to measure the bending and torsion stresses acting on a robot wrist [20].

The wrist force sensor provides force measurement along the three axes of a coordinate system defined at the center of the force sensor and torque measurement about those three axes. The load cell and its connector to the wrist of the robot are machined from a single block for stability. The three force readings and the three torque readings provide useful information for fine manipulation of objects and to detect contact forces with external objects. A wrist force sensor should be compact and of low weight as it has to be mounted on end effectors of manipulators. Other desirable features are high stiffness, good linearity and low hysteresis.

3.4 Sensor Data Fusion

As robots get equipped with an increasing number of sensors (visual, tactile, infrared imaging, laser range finding etc.), we need to address the issue of how best to utilize all the information provided by the sensors. One approach is to use the data of a single most reliable sensor for each parameter of interest. The selection of the single sensor whose data will be used is based on sensor reliability, operating limits and operating cost. An alternative approach is the fusion of all sources of data into one model of the world using the knowledge of the reliability of the information from each sensor. Sensor data fusion is an actively researched field. Several statistical methods have been developed which can *fuse* the readings from multiple sensors into a single piece of information, which is more reliable than

any single reading, if the detailed knowledge of the error statistics of each sensor is available [22]. Many least squares techniques also have been proposed for sensor data fusion.

3.5 Conclusion

So far, the main motivation for studies of the human nervous system in general and the brain in particular came from a psychological and medical point of view. Recent research in sensory systems for robotic applications has also generated interest in the study of the human senses. This multiple approach to understanding the complexities of the human nervous system may soon provide enough knowledge to develop sensors having human skin like properties and to develop the kinesthetic sense of robots to efficiently utilize the contact force information to achieve complex tasks.

Chapter 4

Crack Detection by Contact Sensing

Detecting cracks in surfaces is a problem with many practical applications. Underground pipes carrying fluids may develop cracks after a period of time. The underground location of the pipes and the presence of fluids inside them make it extremely difficult for manual inspection. Similarly manual inspection of ship hulls is a difficult and time consuming process (done either by sending human divers for underwater inspection or by dry-docking of the ships). An automated inspection system which can perform inspection of surfaces and report the presence of cracks will therefore be of great benefit. In this chapter, we propose a robotic system which utilizes force sensing to *feel* surfaces and detect the presence of cracks.

Information about the surface contour, in many situations, can be obtained by vision. Even though high resolution cameras coupled with efficient image processing software enable fast data gathering and processing compared to a tactile system, vision cannot be employed in all situations. In areas of low visibility, such as underwater environments, or sludge filled areas, we need alternative methods to explore surfaces. Even in areas of normal visibility, it is difficult to detect small depressions and bumps in surfaces. As pointed out in [27], psychological experi-

ments have indicated that the human tactile system is a fast and accurate object recognition device. Drawing on this information, researchers are working towards building a robotic tactile recognition system.

Surface reconstruction using a traditional tactile array sensor suffers from low force resolution and low signal to noise ratio due to mechanical cross talk. In addition, a major problem associated with using a tactile array is the difficulty of maintaining stable planar contact with arbitrary surface contours. The above factors coupled with the fragile nature of tactile sensors make them unsuitable for use in rough environments. Applications such as inspecting the surfaces of ship hulls (or pipes) at high speeds place a great demand on the ruggedness of the system employed.

In this chapter, we describe a system for detecting cracks by maintaining a point contact of the tip of a robot manipulator with the object surface and interpreting force and torque data as the tip of the robot moves. We use a linear potentiometer to achieve a compliant end-effector with a point contact. The potentiometer is fixed to the end of the end-effector of the robot, and raster scan is employed to scan any surface. The potentiometer provides compliance as well as position information. This can help in the general contour reconstruction problem as well as in the specific application of crack detection. The use of a single such probe may be too slow to scan large surface areas, but the surface scan time can be reduced by having a one-dimensional array of such potentiometer probes sweep over the surface. Such a sensor is rugged enough to be used in rough contact areas.

We collect force information with a wrist mounted force/torque sensor. Many researchers have considered the use of force sensing for surface feature extraction. The use of force measurements to determine contact geometries is discussed in [23]. Shape recovery from robot-tracking using force feedback is discussed in [2].

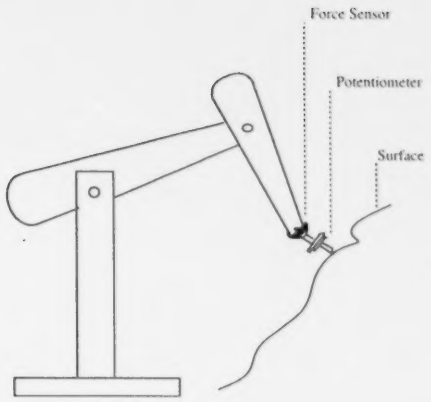

Figure 4.1: Schematic diagram of the robot with sensors.

Our work differs from [2] in that we use the *local* force information at the tip of the end-effector to detect cracks in surfaces, rather than using the force information at the joints along with the joint position information to recover the shape of the contour. Some of the issues related to force sensing while sliding along surfaces are considered by Hemami and Goddard in [13].

The chapter is organized as follows. Section 4.1 describes the system used for our experiments. The mathematical model of the system and its parameter estimation are described in sections 4.2 and 4.3. Section 4.4 describes the experimental results.

4.1 System Description

The robot used in the experiments is a PUMA 260 which is a six degree of freedom industrial robot. Figure 4.1 shows a schematic diagram of the robotic manipulator with a wrist mounted force sensor and a spring return potentiometer.

The potentiometer used is one of the 9600 series of miniaturized spring-return

linear position sensor modules manufactured by Duncan Electronics. Each module is basically a spring-return linear potentiometer housed in a plastic casing with a plastic tip extending out. The total mechanical travel is 26.9 mm.

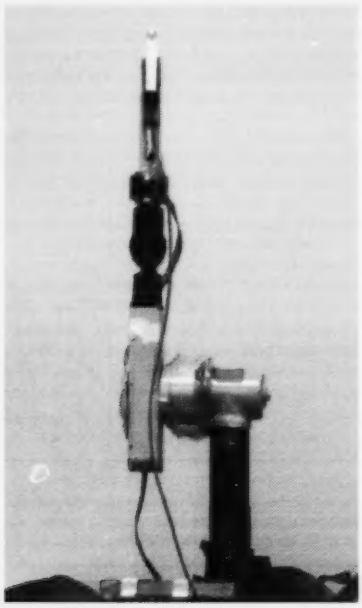

Figure 4.2: The photograph of the robot with wrist mounted sensors.

The force sensor, manufactured by Zebra Robotics Inc., is a six axis force sensor capable of measuring a complete 6x1 force/torque vector in Cartesian coordinates. It is a cylindrical unit consisting of a bending beam flexure instrumented with six pairs of semiconductor strain gauges and a six-channel data acquisition system. The six digitized strain readings are required to be multiplied by a calibration matrix in the user's program to produce a 6x1 vector of three force values and three torque values. Its sensitivity is 25 grams, dynamic range is 1:1024 and the conversion time is 1.0 millisecond per complete strain vector reading.

If the robot traverses any surface, with the tip of the potentiometer in contact with the surface, it encounters large contact forces due to sliding friction. Vibrations are also induced in the system. It is possible to slide across surfaces only at

very slow speeds. The large amount of sliding friction can be reduced to negligible rolling friction by attaching a small roller ball at the tip of the potentiometer. We used two metallic ball bearings of different diameters (12 mm and 15.9 mm) in our experiments. The robot used in the experiments is shown in Figure 4.2. A closeup showing the robot wrist with the sensor assembly is shown in Figure 4.3.

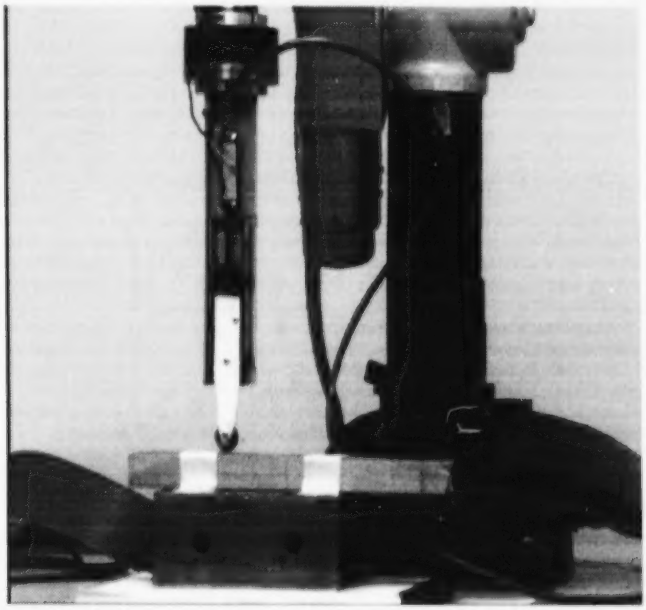

Figure 4.3: A closeup of the wrist with the sensors.

4.2 Modeling of a Linear Potentiometer

The linear position sensor module consists of a spring return potentiometer. Its mathematical model is shown in Figure 4.4 [16, 31]. K is the spring constant (a measure of the spring stiffness), C is the damping coefficient and M is the mass of the movable portion of the sensor module.

When a linear spring is stretched, there is a constant displacement per unit of force applied until a certain point, beyond which the spring becomes nonlinear. We assume operation in the linear range. All practical springs have inertia and

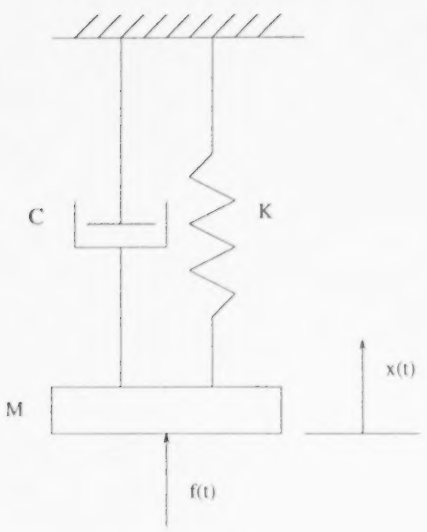

Figure 4.4: Spring-Damper model.

damping. The damping is modeled by the translational damper or dashpot and the inertia is modeled by mass. Here, the mass of the spring and the mass of the extended part of the sensor module constitute the mass M.

When the potentiometer tip is forced to move over a surface which has a positive slope, the tip is forced inwards by the reaction force from the surface acting on the tip. This force provides the acceleration of the mass and is opposed by the spring and damper. The equation of the system can be written as follows:

$$f(t) = M\ddot{x}(t) + C\dot{x}(t) + Kx(t) \tag{4.1}$$

where $\dot{x}(t)$ is the first order time derivative of $x(t)$ and $\ddot{x}(t)$ is the second order time derivative of $x(t)$.

If force were the input quantity, the above differential equation could be solved to express $x(t)$ as a function of $f(t)$. In our case, the potentiometer tip is traversing a surface whose height is varying. Therefore, $x(t)$ varies, and the reaction force varies according to the above equation.

When the robotic arm moves across a crack, the tip loses contact with the

surface. The tip will lose contact with the surface at all the edges of the surface as well. A priori knowledge of the edges in the surface contour being followed will have to be used to distinguish the cracks from the edges. Figure 4.5 shows a spring which has just moved off the surface while sliding across it.

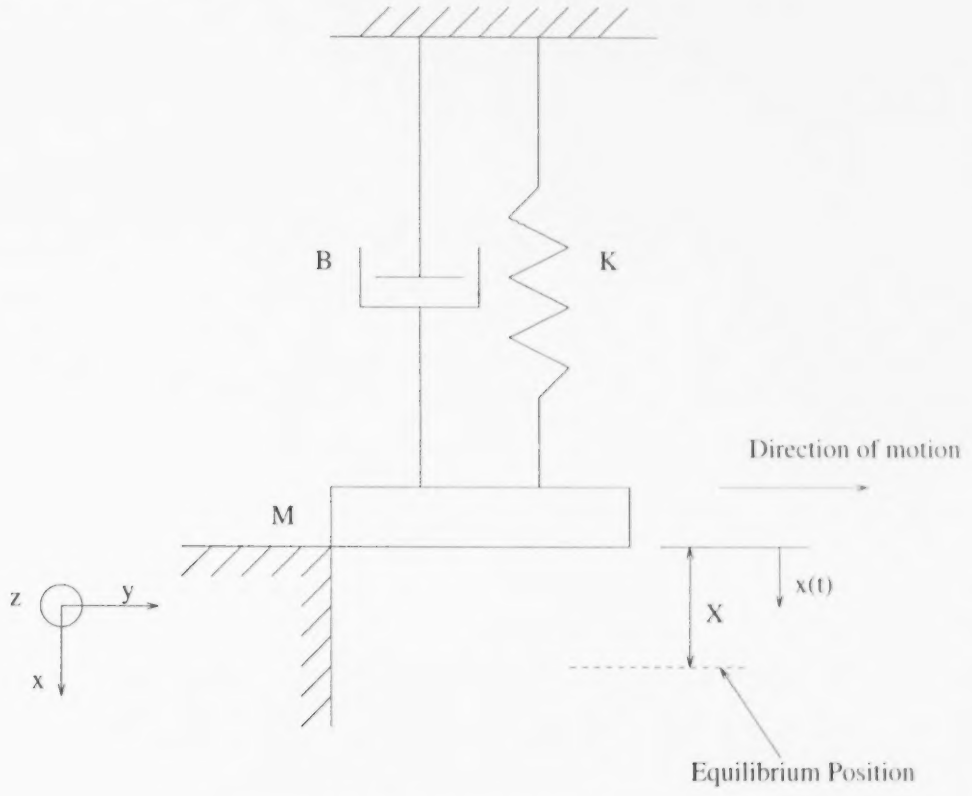

Figure 4.5: Spring extension into a crack.

In such a case, the compressed spring starts expanding (free response). Let X be the initial compression (deflection from equilibrium). The force in the spring $K(X - x_1(t))$ provides acceleration to the mass and is opposed by damping. We get the following equation:

$$K(X - x_1(t)) = M\ddot{x_1}(t) + C\dot{x_1}(t)$$

It can be rearranged as

$$M\ddot{x_1}(t) + C\dot{x_1}(t) + Kx_1(t) = KX$$

Taking Laplace transforms and simplifying, we obtain

$$Y(s) = \frac{KX}{s(Ms^2 + Cs + K)} \tag{4.2}$$

Using partial fraction expansion and taking the inverse Laplace Transforms, we get

$$x(t) = A_1 + A_2 e^{r_1 t} + A_3 e^{r_2 t}$$

where r_1 and r_2 are the roots of the quadratic equation $Ms^2 + Cs + K = 0$, and A_1, A_2, A_3 are as follows:

$$\begin{aligned} A_1 &= \frac{KX/M}{r_1 r_2} \\ A_2 &= \frac{KX/M}{r_1(r_1 - r_2)} \\ A_3 &= \frac{KX/M}{r_2(r_2 - r_1)} \end{aligned} \tag{4.3}$$

The transfer function of a pure second order system can be represented by the following equation.

$$G(s) = \frac{1}{s^2 + 2\zeta\omega s + \omega^2} \tag{4.4}$$

where ζ is the damping ratio and ω is the natural frequency. The second order system is said to be underdamped if $\zeta < 1$, critically damped if $\zeta = 1$ and overdamped if $\zeta > 1$. Since the laplace transform of a step function is $1/s$, the step response of a second order system is given by,

$$G(s) = \frac{1}{s(s^2 + 2\zeta\omega s + \omega^2)} \tag{4.5}$$

Comparing Equations 4.5 and 4.2, we get expressions for the ζ and ω of the spring-mass-damper system. The plot in Figure 4.6 shows the spring extension in free response for various damping conditions.

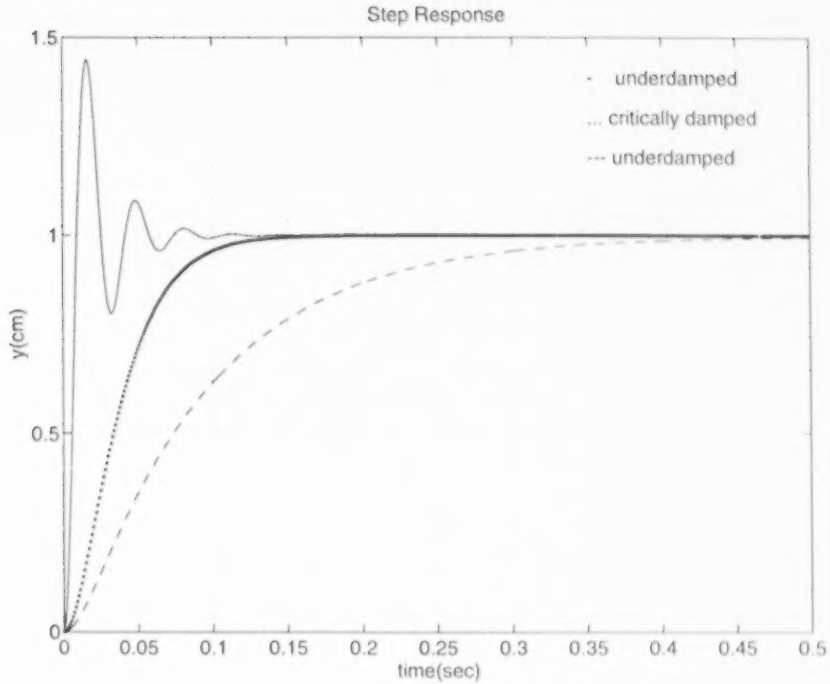

Figure 4.6: Step response of the spring.

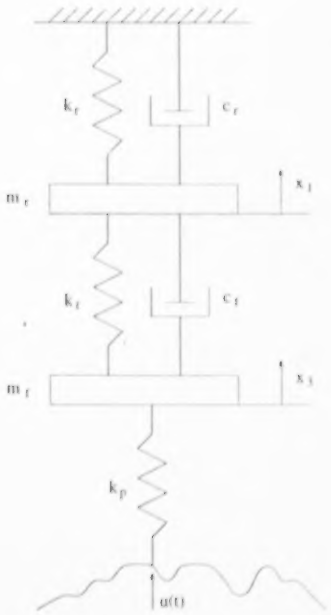

Figure 4.7: System model.

4.3 Model Including the Force Sensor

Of the six axes of the force sensor, we are interested in the z-component of force. The frame of reference is shown in Figure 4.5. The force sensor is modeled as a simple spring-damper system and cascaded with the potentiometer model and a spring-mass-dashpot model of the robot wrist as shown in Figure 4.7. The potentiometer's mass and damping are negligible and therefore it is represented as an ideal spring.

The system parameters are as follows:

m_r: The mass of the robot wrist.

m_f: The mass of the force sensor.

c_r: The damping coefficient of the robot wrist.

c_f: The damping coefficient of the force sensor.

k_f: The spring constant of the robot wrist.

k_f: The spring constant of the force sensor.

k_p: The spring constant of the potentiometer.

The state variables are:

x_1: The displacement of m_r.

x_2: The velocity of m_r ($x_2 = \dot{x}_1$).

x_3: The displacement of m_f.

x_4: The velocity of m_f ($x_4 = \dot{x}_3$).

The input to the system is the terrain elevation expressed as a function of time, $u(t)$. The reading of the force sensor is $K_f(x_3 - x_1)$.

From an inspection of Figure 4.7, the following equations can be written.

$$\begin{aligned} k_p(u(t) - x_3) &= m_f(\dot{x_4}) + k_f(x_3 - x_1) + c_f(x_4 - x_2) \\ k_f(x_3 - x_1) &= m_r(\dot{x_2}) + c_f(x_4 - x_2) + k_r(x_1) + c_r(x_2) \end{aligned}$$

The dynamic equations describing the system behaviour can be represented as follows:

$$\begin{bmatrix} \dot{x_1} \\ \dot{x_2} \\ \dot{x_3} \\ \dot{x_4} \end{bmatrix} = \begin{bmatrix} 0 & 1 & 0 & 0 \\ \frac{-(k_f+k_r)}{m_r} & \frac{(c_f-c_r)}{m_r} & \frac{k_f}{m_r} & \frac{-c_f}{m_r} \\ 0 & 0 & 0 & 1 \\ \frac{k_f}{m_f} & \frac{c_f}{m_f} & \frac{-(k_p+k_f)}{m_f} & \frac{-c_f}{m_f} \end{bmatrix} \begin{bmatrix} x_1 \\ x_2 \\ x_3 \\ x_4 \end{bmatrix} + \begin{bmatrix} 0 \\ 0 \\ 0 \\ \frac{k_p}{m_f} \end{bmatrix} u(t) \qquad (4.6)$$

The above model can be simplified by considering the fact that the stiffness coefficient of the wrist is very high compared to the other two stiffness coefficients. The simplified model is redrawn in Figure 4.8.

The dynamic equations of the system can now be represented as follows:

$$\begin{bmatrix} \dot{x_1} \\ \dot{x_2} \end{bmatrix} = \begin{bmatrix} 0 & 1 \\ \frac{-(k_f+k_p)}{m_f} & \frac{-c_f}{m_f} \end{bmatrix} \begin{bmatrix} x_1 \\ x_2 \end{bmatrix} + \begin{bmatrix} 0 \\ \frac{k_p}{m_f} \end{bmatrix} u(t) \qquad (4.7)$$

From the above equation, we can write,

$$m_f\dot{x_2} = -(k_p + k_f)x_1 - c_f x_2 + k_p u(t) \qquad (4.8)$$

Taking the Laplace transform of the above equation we get,

$$\frac{X_1(s)}{U(s)} = \frac{\frac{K_p}{m_f}}{s^2 + \frac{C_f}{m_f}s + \frac{(K_p+K_f)}{m_f}} \qquad (4.9)$$

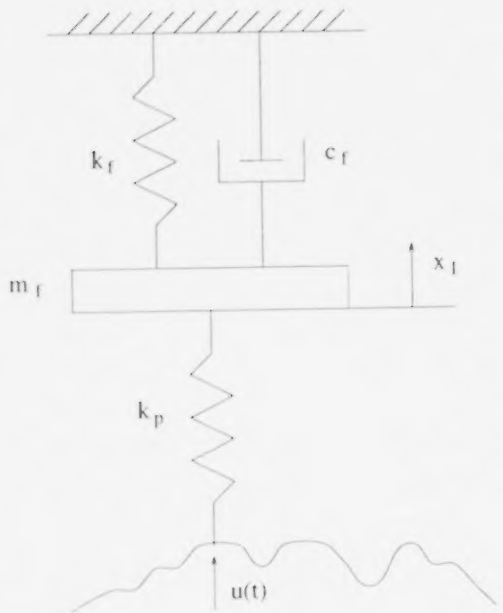

Figure 4.8: Simplified system model.

This equation can be rewritten as

$$\frac{X_1(s)}{U(s)} = \frac{K}{s^2 + 2\zeta\omega_n s + \omega_n^2} \tag{4.10}$$

where,

$$\begin{aligned} k &= k_p/m_f \\ \omega_n &= \sqrt{(k_p + k_f)/m_f} \\ \zeta &= c_f/2\sqrt{m_f(k_p + k_f)} \end{aligned}$$

ω_n is the natural frequency and ζ is the damping ratio. The force sensor reading in the direction along the axis of the potentiometer is given by

$$f = k_f x_1 \tag{4.11}$$

Using equations 4.9 and 4.11, we can relate the force sensor reading f to the terrain elevation $u(t)$. The determination of the system parameters of the model is discussed below.

4.3.1 System Parameter Estimation

When the system parameters in any model are not directly measurable, they can often be determined by making use of step response data [24]. If for any reason, it is not possible to provide the system with a step input, sinusoidal or pulse testing methods can be used. Statistical identification techniques [7] and advanced optimization codes for parameter estimation can also be used. In our case, we can easily provide a step input to the system. A step input can be provided to the force sensor/potentiometer assembly in either of the following ways:

- The force sensor and potentiometer can be mounted on the robot wrist as shown in Figure 4.1 and the robot can be moved vertically down to make contact with a hard surface in a short time.
- The potentiometer can be mounted on the force sensor which can be placed on a rigid surface. The potentiometer tip can then be fully compressed and released instantaneously. This method proved to be better at approximating a step input, since it is difficult to move the robot with sufficient speed to approximate a step input. At slow speeds, the input turns out to be a ramp.

Taking the inverse laplace transform of Equation 4.9, we can write

$$x_1(t) = k\ \mathcal{L}^{-1}(F(s)) \tag{4.12}$$

where $F(s) = U(s)/(s^2 + 2\zeta\omega_n s + \omega_n^2)$.
From Equation 4.11 and 4.12 we get

$$f(t) = k_f k\ \mathcal{L}^{-1}(F(s)) \tag{4.13}$$

A step input can be provided and $f(t)$ obtained from the force sensor readings. The quantity $\mathcal{L}^{-1}(F(s))$ can be evaluated and then, $k_f k$ can be calculated using

Equation 4.13. We now discuss the determination of the second order model parameters ζ and ω_n.

Several graphical methods exist to determine the second order model parameters using step tests. Oldenbourg and Sartorious [17] and Harriott [12] have provided techniques for the estimation of the time constants of overdamped systems. An overdamped second order model can be represented as follows:

$$G(s) = \frac{Ke^{-\theta s}}{(\tau_1 s + 1)(\tau_2 s + 1)} \tag{4.14}$$

Oldenbourg and Sartorious' method, as presented in [18], can be illustrated by considering Figure 4.9, which shows an arbitrary step response. A tangent is drawn to the point of inflection. T_c and T_a are measured as shown in Figure 4.9.

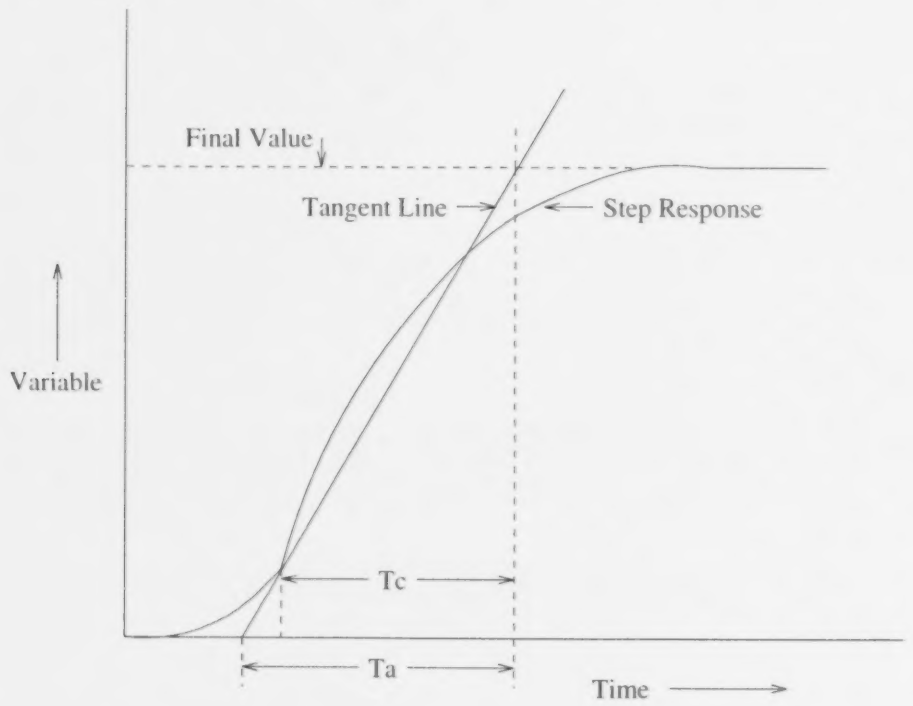

Figure 4.9: Oldenbourg-Sartorius method.

The time constants, τ_1 and τ_2, are obtained from the following equations:

$$T_c = \tau_1 + \tau_2 \tag{4.15}$$

$$\frac{T_c}{T_a} = (1+x).x^{x/(1-x)} \tag{4.16}$$

where x is τ_1/τ_2.

Cox *et al.* [5] extended the Oldenbourg-Sartorius method to determine the dead time (transportation delay). The Oldenbourg-Sartorius method cannot be applied to underdamped systems, nor can it be used for all overdamped systems. It requires the estimation of a point of inflection, which makes it difficult to be used with noisy data [24]. Harriott [12] proposed another approach to estimate the two time constants of an underdamped second order model which does not require the estimation of a point of inflection. Seborg *et al.* [24], point out that Harriot's method becomes less accurate as τ_2/τ_1 approaches unity.

Smith's Method

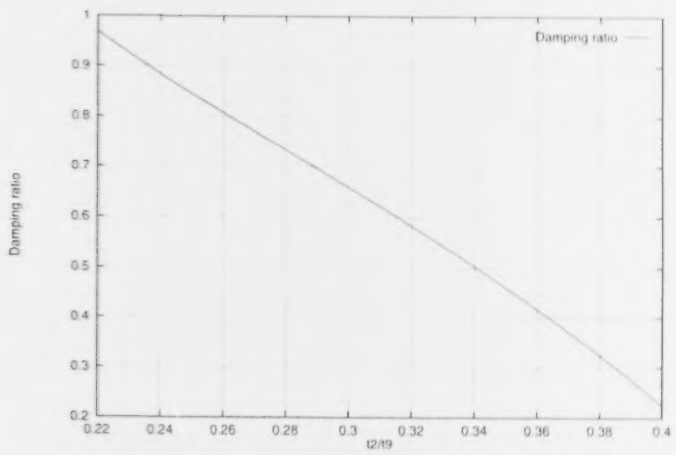

Figure 4.10: Smith's method: Damping ratio Vs Time ratio.

The above methods can be applied only to overdamped systems. Smith and Murrill [26] proposed a method for underdamped systems. This method is not applicable to systems with dead time. Later, Smith and associates [18, 25], presented a method to estimate the parameters of a second order model with dead

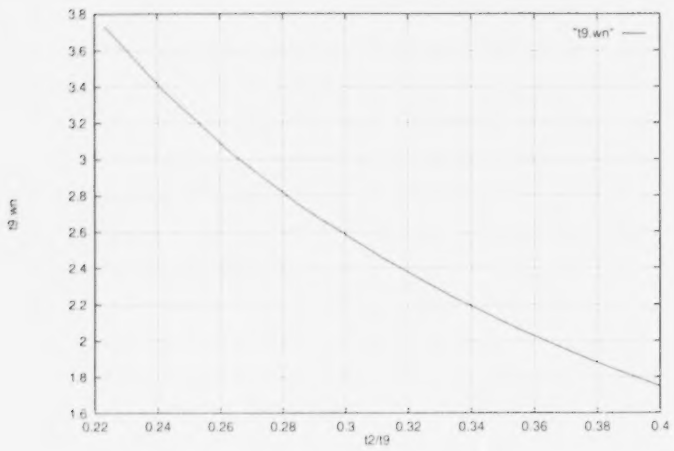

Figure 4.11: Smith's method: Natural frequency Vs Time ratio.

time, applicable to either underdamped or overdamped systems. This method, from now onwards referred to as Smith's method, is easy to use and reasonably accurate. Smith's method uses Cox's method [5] to determine dead time, and the following method to determine the system parameters. A pure second order model for both overdamped and underdamped systems can be represented by a natural frequency (ω_n) and a damping ratio (ζ). The transfer function, G(s) is given by:

$$G(s) = \frac{1}{\frac{s^2}{\omega_n^2} + \frac{2\zeta s}{\omega_n} + 1} \tag{4.17}$$

Let t_2 and t_9 be the times at which the normalized response reaches 20 percent and 90 percent of the final value, respectively. The values of the normalized response at t_2 and t_9 will be $t_2\omega_n$ and $t_9\omega_n$. The ratio of these two values (t_2/t_9) is independent of w_n, and only depends on ζ. The values of ζ, $t_9\omega_n$ and t_2/t_9 are tabulated by reading t_2 and t_9 and $t_9\omega_n$ for various values of ζ and the graphs shown in Figure 4.10 and Figure 4.11 can be plotted [18].

Smith's method consists of obtaining t_2/t_9 from the step response of a second order system and determining the value of ζ from the Figure 4.10. The value of

ω_n can be calculated by finding the values of t_9 from the step response data and $t_9\omega_n$ from Figure 4.11. The choice of 20% and 90% points is arbitrary. Any two points on the response curve could be chosen for this method.

Application of Smith's Method to Our Model

The potentiometer module is attached to the force sensor, which is placed on a rigid support.The value of the force sensor reading in the direction along the axis of the potentiometer module is monitored as the potentiometer is fully compressed and released. Figure 4.12 shows the smoothed step response data.

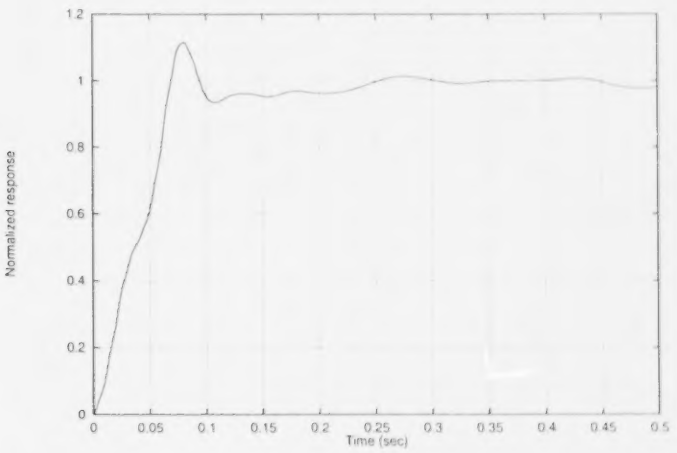

Figure 4.12: Smoothed step response data.

From Figure 4.12, we note that $t_2/t_9 = 0.295$. Applying Smith's method to the above data, we get $\zeta = 0.677$ and $\omega_n = 43.45s^{-1}$. Using these values in Equation 4.17, the normalized step response of the model is plotted in Figure 4.13 along with the actual step response. We see that Smith's method gives us a fairly good approximation.

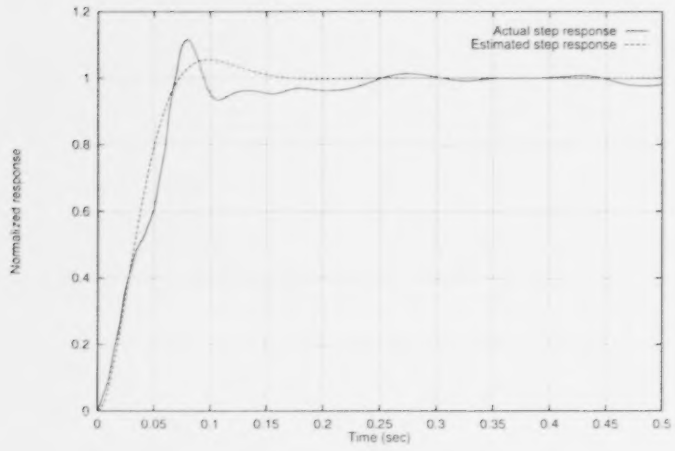

Figure 4.13: Actual data and the model's approximation .

4.4 Experimental Results

The sensors are mounted on the end-effector of the PUMA 260 as shown in Figure 4.1. The specimen piece whose surface has to be examined for the presence of cracks is placed horizontally within the robot's work space. The robot is moved in a straight line trajectory such that the wheel at the tip of the potentiometer rolls across the surface. Inspection of any surface consists of a sufficient number of parallel horizontal scans. The force sensor values from each horizontal scan are stored, and the process is continued till the entire surface is scanned. In our experiments, we perform only a single horizontal scan across each surface to illustrate the process.

The orientation of the force sensor is such that the value of the force in the vertical direction increases positively when the tip moves into a crack and vice versa when it encounters a bump. A crack or depression in the surface therefore shows up as a pair of adjacent edges (a rising edge followed by a falling edge) in the vertical force signal. Figure 4.14 shows the coordinate frame assignment of the wrist force-torque sensor. Our mathematical model corresponds to the vertical

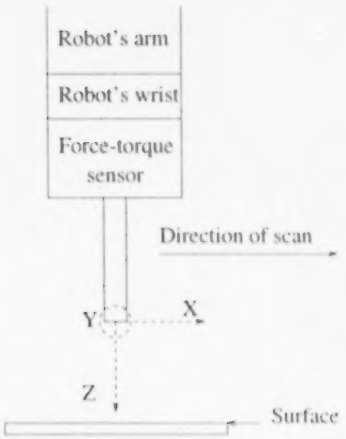

Figure 4.14: The coordinate frame assignment of the force-torque sensor.

force response, i.e., the force along the z-axis, f_z. We also observe the signal of the torque about the y-axis, t_y.

For the purpose of our experiments, we use flat, rectangular slabs of plexiglass with different kinds of grooves to simulate different kinds of cracks. The grooves are all cut at exactly 200 mm from the end of the slab where the robot starts its scan. The force sensor takes readings at the rate of 400 per second. In order that at least one reading be taken while traversing over a crack of width w, the velocity with which the robot's tip moves across the surface has to be less than $400w$ m/s. The smallest crack width in our specimen pieces is 1 mm limiting our maximum scan velocity to 0.4 m/s.

4.4.1 The Vertical Force Response

The orientation of the force sensor (Figure 4.14) is such that the value of the force in the vertical direction increases positively when the tip moves into a crack and vice versa when it encounters a bump. A crack or depression in the surface therefore shows up as a rising edge followed by a falling edge in the vertical force signal (f_z). A typical f_z signal obtained by scanning a surface with a 6 mm wide

and 3 mm deep crack at 200 mm from one end is shown in Figure 4.15. The scanning velocity (the lateral velocity of the robot's tip) is 0.2 m/s in this case.

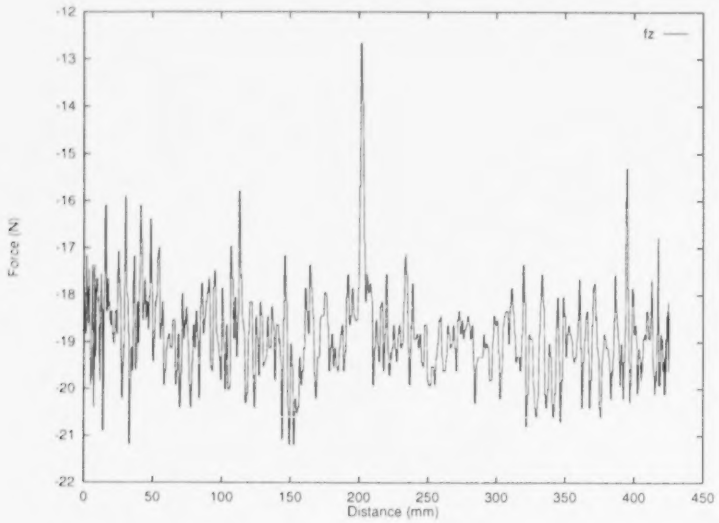

Figure 4.15: A typical vertical force signal.

4.4.2 Noise

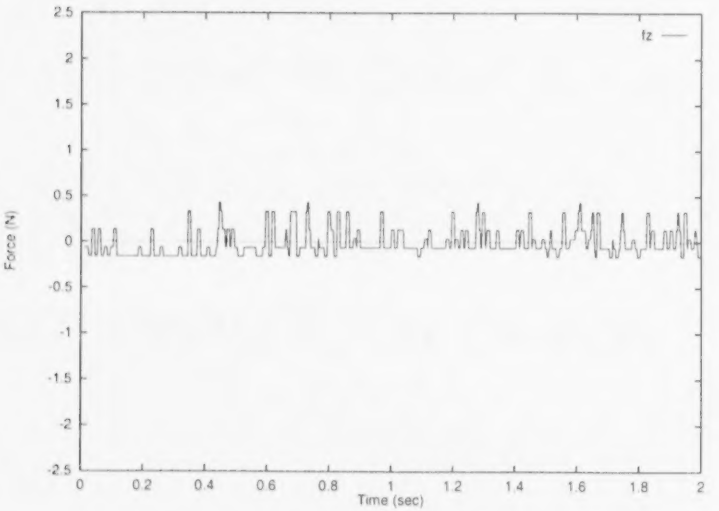

Figure 4.16: The force signal when the robot is stationary.

Ideally, the vertical force signal should be a straight line at all points corresponding to a flat surface. However, we observe considerable fluctuations in the signal even at points corresponding to a flat surface in Figure 4.15. The following simple experiments help in identifying the source of these fluctuations. Figure 4.16 shows the f_z signal when the robot is stationary. The f_z signal in this plot and the next two are scaled to show variations about zero. Ideally this signal should be a straight line. However, we observe a peak to peak variation of approximately 0.6 N. This is the inherent noise in the sensor.

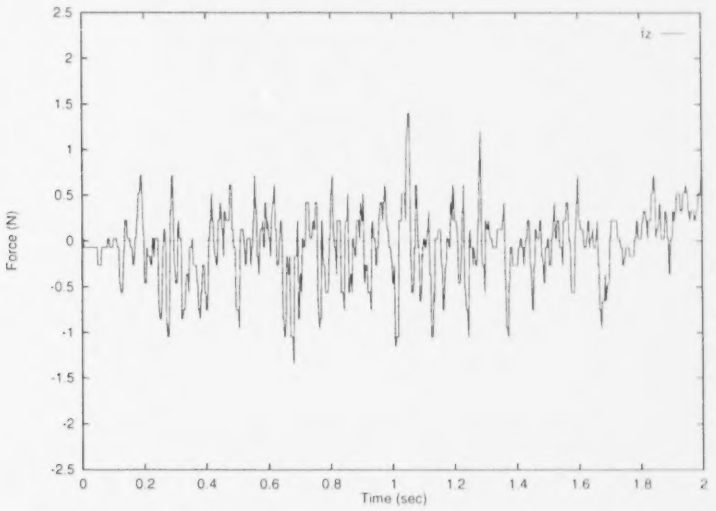

Figure 4.17: The force signal when the robot is moving without touching any surface.

Figure 4.17 shows the f_z signal obtained when the robot is moving in a straight line path without touching any surface. We now observe a peak to peak variation of approximately 2.8 N. This increased amount of fluctuation is probably due to (a) the fact that the robot is unable to travel in a straight line path accurately and (b) the sensor reading getting affected by electric currents in the joint motors.

Figure 4.18 shows the f_z signal obtained when the robot is moving in the same straight line path as before but now with its tip in contact with a flat surface.

The higher peak to peak variation (4 N) in this case is due to (a) even higher load currents in the joint motors and (b) the forces arising due to the contact of the robot's tip with the hard surface.

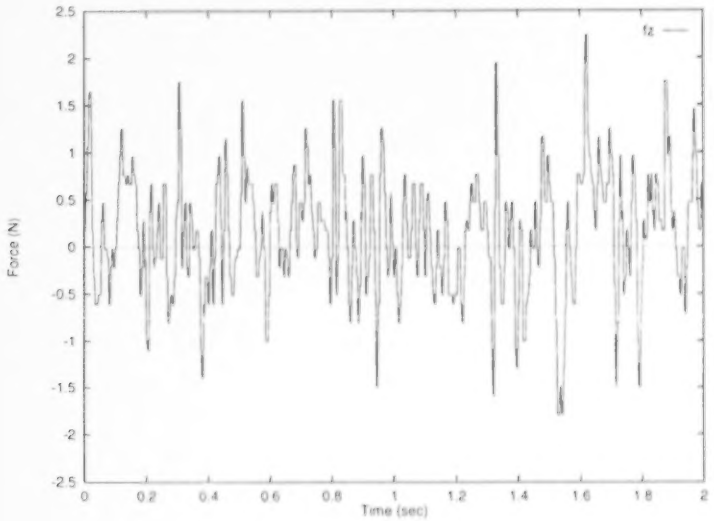

Figure 4.18: The force signal when the robot is moving with its tip in contact with a flat surface.

The Effect of Varying the Wheel Diameter

We use two different wheels at the end of the sensor assembly and collect data over the same surfaces to observe the effect of varying wheel diameter on the detectability of cracks.

The force reading in the vertical direction is dependent on the vertical displacement of the tip of the sensor assembly. If the crack is such that its width is larger than the diameters of the two wheels being compared, the vertical displacement of the tip of the sensor assembly is independent of the wheel diameter. We shall consider the case where the width of the crack is less than the wheel diameters. The vertical displacement d is then a function of the radius r of the wheel and the width w of the crack (Figure 4.19).

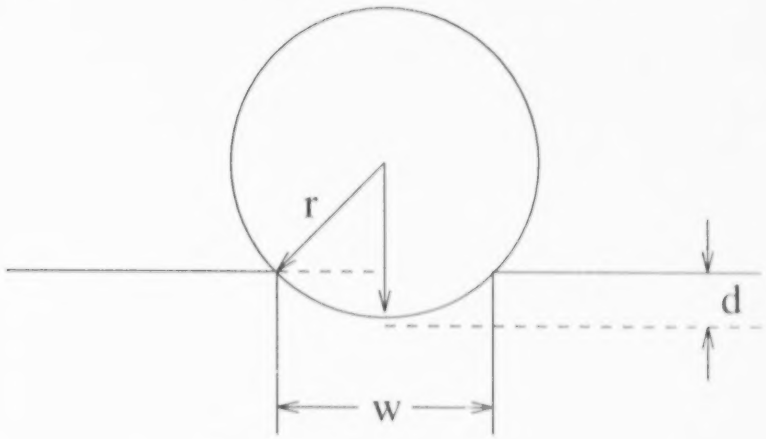

Figure 4.19: The effect of wheel diameter on the input to the sensor.

The maximum vertical displacement of the tip of the sensor assembly, d, is given by

$$d = r - \sqrt{r^2 - \left(\frac{w}{2}\right)^2} \tag{4.18}$$

For a given width, d depends only on r.

The two wheels used in our experiments have radii of 6 mm and 7.95 mm respectively. Figure 4.20 shows the vertical force responses for the two wheels when the robot's tip is rolled across a surface with a triangular crack, 3 mm deep and 6 mm wide. The scanning velocity is 0.2 m/s in each case. The force response with the wheel of smaller diameter is slightly higher than that with the wheel of larger diameter.

Figure 4.21 shows the vertical force response when the robot's tip is rolled across a surface with a wide crack, 3 mm deep and 20 mm wide, with 45° end slopes. The scanning velocity is 0.2 m/s in each case. In this case, as expected, there is no difference in the magnitude of the force response obtained since the input to the sensor is the same in both cases, as the width of the crack is larger than the diameters of the wheels.

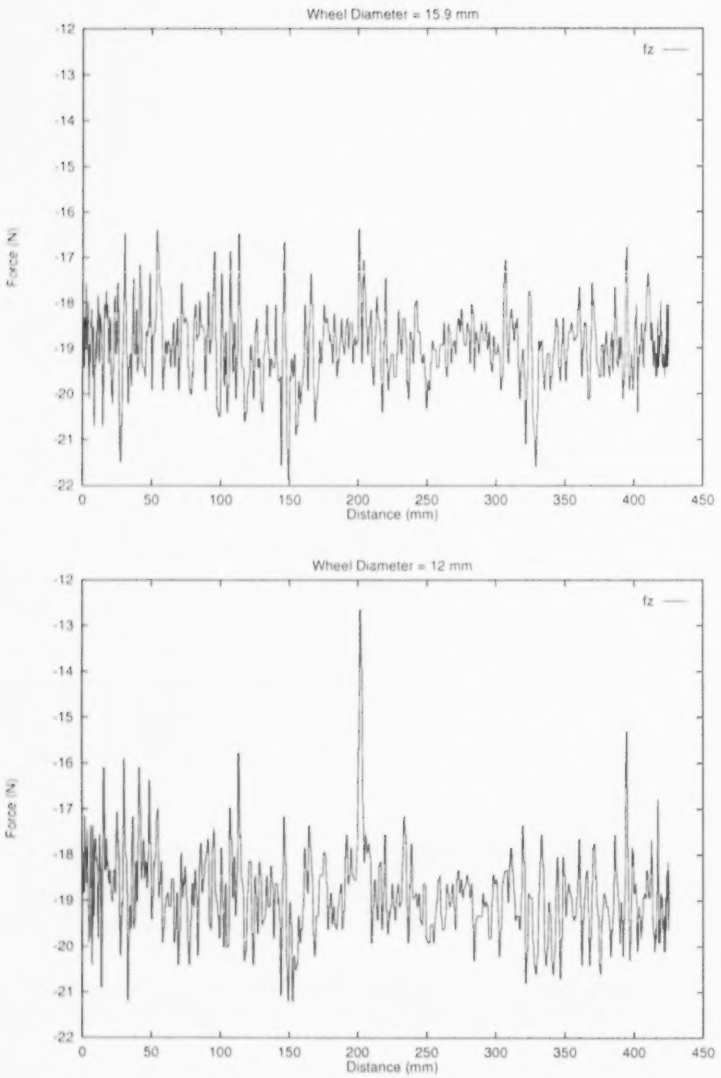

Figure 4.20: The effect of wheel diameter on the force response when the width of the crack is less than the wheel diameters.

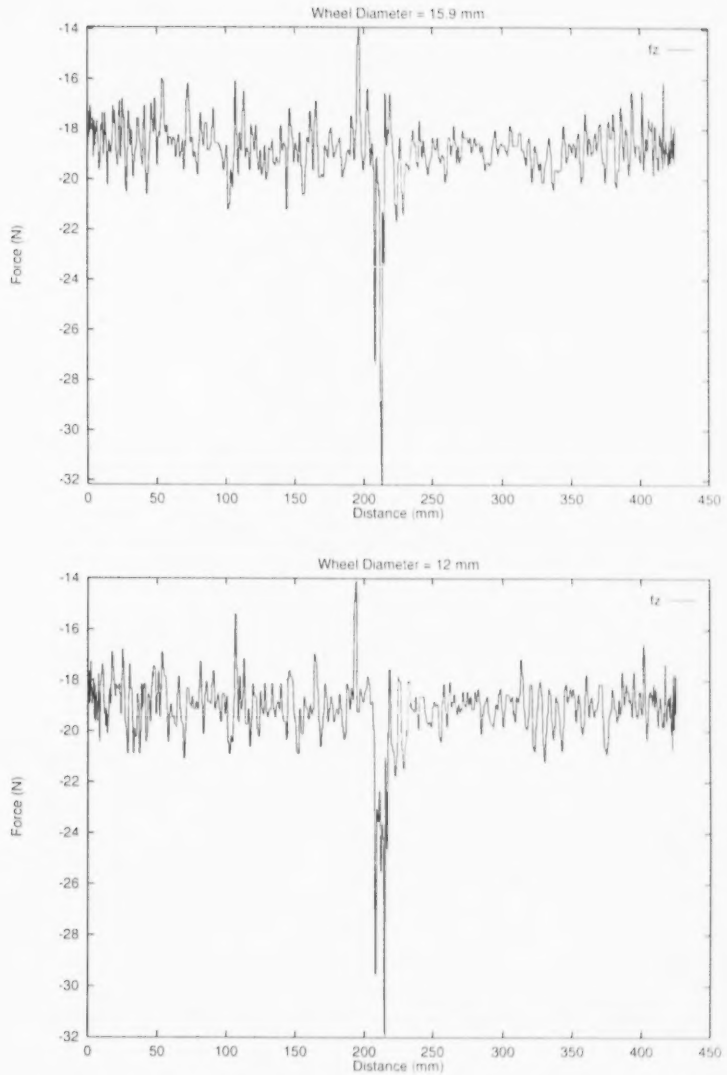

Figure 4.21: There is no effect of wheel diameter on the force sensor when the width is larger than the wheel diameters.

The Effect of Increasing the Dimensions of the Crack

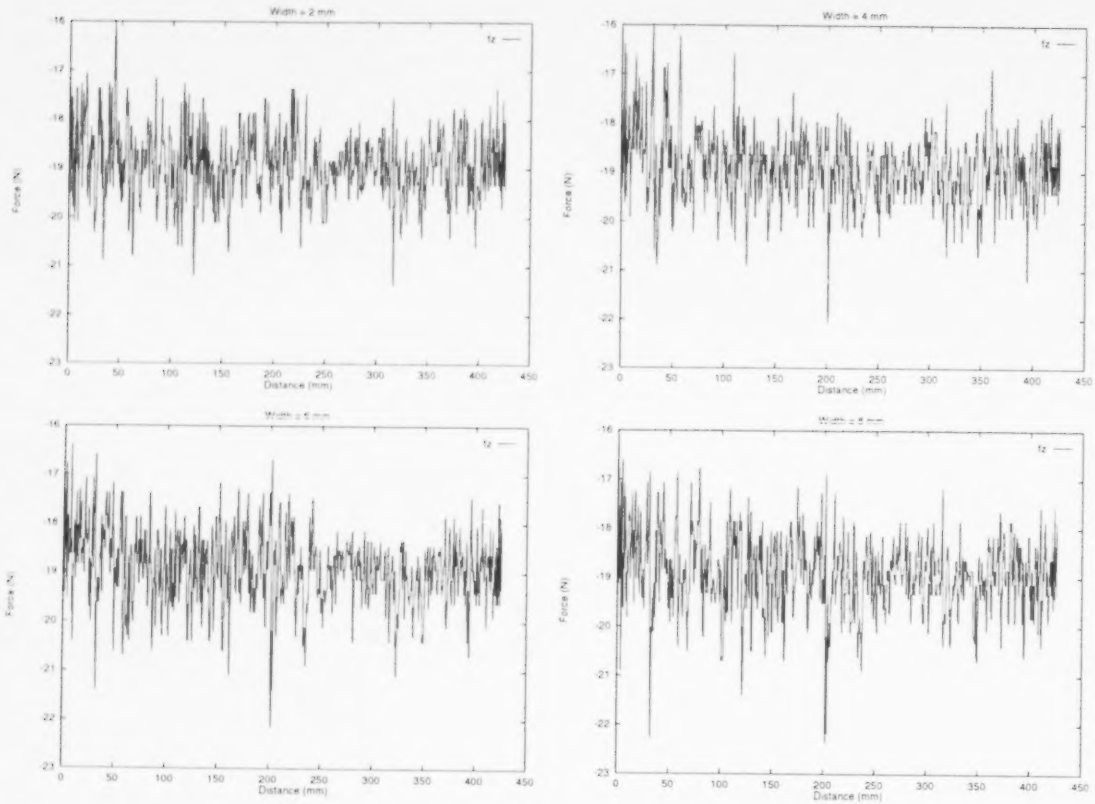

Figure 4.22: The vertical force response is higher for wider cracks.

When the robot's tip rolls across a surface with a crack, the vertical displacement of the tip for a given wheel is dependent on the dimensions of the crack. Equation 4.18, which gives the relation between the vertical displacement d, the radius of the wheel r and the width of the crack w, is applicable when $w <= 2r$. According to this equation, d, the input to the force sensor, increases with increasing crack width and therefore the magnitude of the force response should increase with increasing crack width. For the case when $w > 2r$, the vertical displacement of the tip of the sensor assembly, and hence the force response (in the vertical direction) of the force sensor depends only on the depth of the crack.

Figure 4.22 shows the vertical force signals for four surfaces with cracks of

widths 2, 4, 6 and 8 mm respectively. The depth of each crack is half its width. The wheel diameter is 12 mm and the scan velocity is 0.1 m/s. In each case, the wheel diameter is smaller than the width of the crack, and therefore there is an increase in the vertical force response (as explained in the previous paragraph).

4.4.3 The Torque about the Sensor's Y-axis

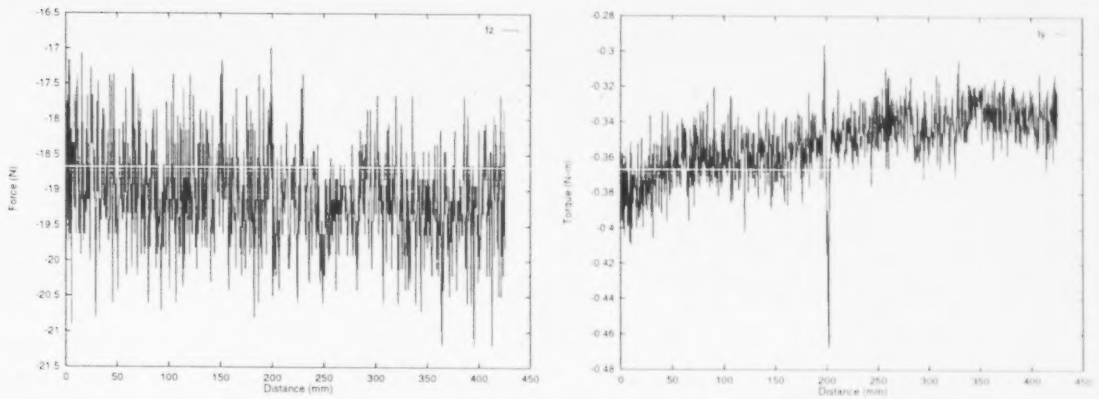

Figure 4.23: The force and torque signals for a crack of width 7 mm and depth 0.5 mm.

The distance from the center of the wheel at the tip of the sensor assembly to the center of the force sensor is 210 mm. The torque t_y is the product of this length and the lateral force acting opposite to the direction of scan at the tip of the sensor assembly. This long moment arm essentially acts as an amplifier and the resultant torque signal is much more useful than the vertical force response in detecting cracks in surfaces. The plots in Figures 4.23, 4.24 and 4.25 show the f_z and t_y signals obtained over surfaces with cracks of different dimensions.

An explanation for the shape of the torque signal is as follows. When the tip of the sensor assembly extends into a crack, there is a decrease in the lateral force at the tip opposite to the direction of motion of the robot's tip. Referring to Figure 4.14, we can see that this corresponds to a decrease in the clockwise torque about the sensor's positive y-axis. The sensor's value increases positively

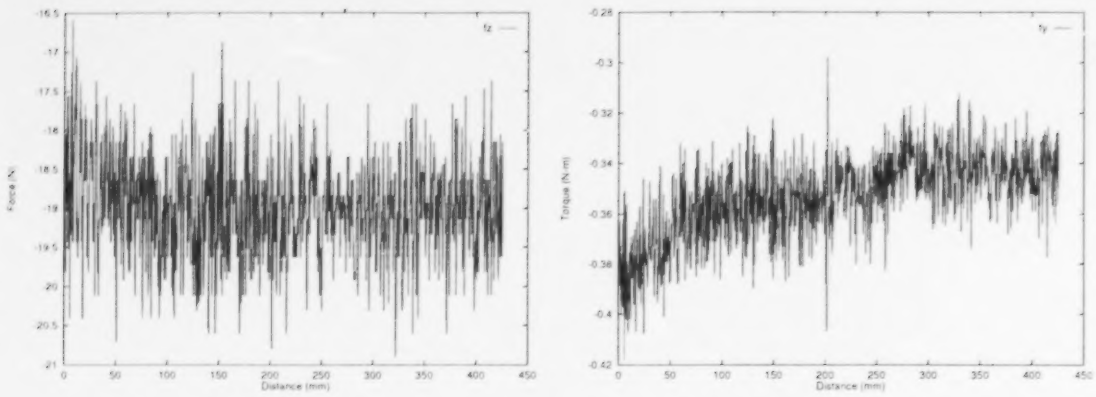

Figure 4.24: The force and torque signals for a crack of width 2 mm and depth 1 mm.

for a decrease in the clockwise torque about the sensor's y-axis. Therefore, we see a rising edge in the torque signal t_y. When the tip hits the other end of the crack, there is an increase in the lateral force at the tip causing an increase in the clockwise torque about the sensor's positive y-axis leading to a falling edge in the t_y signal. We can use any edge detection technique to determine the location and width of the crack.

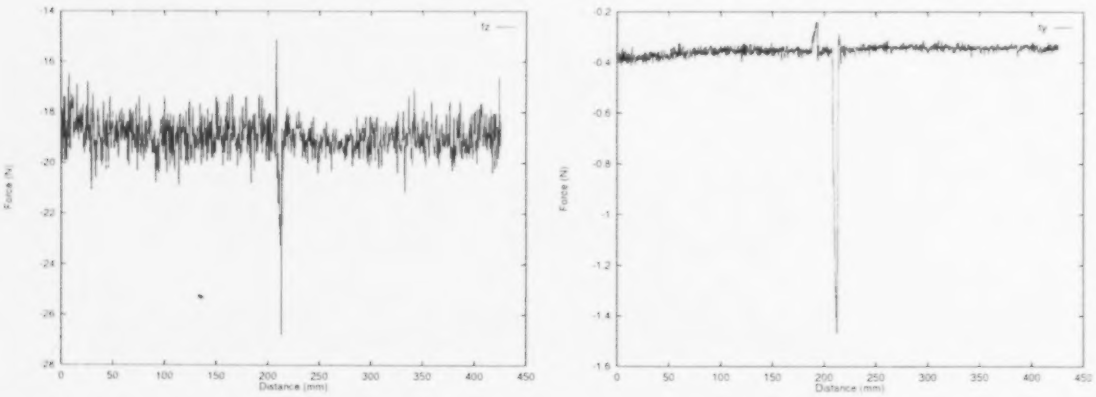

Figure 4.25: The force and torque signals for a crack of width 20 mm and depth 3 mm.

Chapter 5

Conclusion

We have a developed a mathematical model of the system which explains the vertical force response of the system. We also need to develop a model to explain the torque signal (the torque about the y-axis of the sensor).

Each horizontal scan across a surface yields a force signal. We have seen that peaks in the force signal correspond to cracks in the surface. Now, a force signal typically consists of large number of maxima and minima. We can think of these as representing cracks at different scales. We need a compact description of the force signal to help us interpret it better. This compact description should consist of elements which correspond to meaningful events in the signal forming case [32]. The meaningful event in our case is the presence of cracks (or bumps). The cracks can be identified as peaks in the force signal which can be easily obtained as *zero crossings* in the first derivative. When we attempt to describe a signal based on its derivatives, we run into the problem of scale, making the task of signal description very difficult.

As pointed out in [32], the derivative operator has to depend on the value of the signal at two or more neighboring points, and the signal description in terms of the second derivative is thus dependent, not only on the value of the signal at any point, but also on the spatial extent of the neighborhood chosen. Thus, any

description of a signal depends on the parameter of scale. In our case, if we choose a small neighborhood, we will be able to get information about small cracks on the surface and if we choose a large neighborhood, small surface perturbations will be left out, but we will be able to identify surface variations of larger magnitude. The use of the scale space approach to give a unified and compact description of the surface across all scales is highly desirable.

The above experiments and discussion centered on detecting and locating cracks in a single scan of the surface. The next task is to integrate the information from multiple parallel scans to determine the spread of the crack on the surface. Another possible area of research is that of "intelligent scan", where we use the information about cracks obtained from previous scans to direct the next scan. This cuts down on total scan time and facilitates the determination of the spread of the crack over the surface.

Bibliography

[1] E. D. Adrian. *The Basis of Sensation.* Christophers, 22, Berners St, London, 1928.

[2] S. Ahmed and C. N. Lee. Shape recovery from robot contour-tracking with force feedback. In *Proc. of the IEEE Int. Conf. on Robotics and Automation*, pages 447–452, 1990.

[3] J. Albus. A model of the brain for robot control, part 3: A comparison of the brain and our model. *Byte*, pages 66–80, August 1979.

[4] J. Case. *Sensory Mechanisms.* The MacMillan Company, New York, 1966.

[5] J. B. Cox, L. J. Hellums, T. J. Williams, R. S. Banks, and G. J. Jr. Kirk. A practical spectrum of ddc chemical process control algorithms. *ISA Journal*, 13(10):70, October 1966.

[6] P. Dario. Tactile sensing for robots: Present and future. In O. Khatib, J. J. Craig, and T. Lozano-Perez, editors, *The Robotics Review 1*, pages 133–146. MIT Press, 1989.

[7] P. Eykhoff. *System Identification: Parameter and State Estimation.* John Wiley and Sons, New York, 1974.

[8] G. T. Fechner. *Elements of Psychophysics.* Rinehart and Winston, New York, 1966.

[9] F. A. Geldard. *The Human Senses.* John Wiley and Sons, New York, 1972.

[10] E. B. Goldstein. *Sensation and Perception.* Wadsworth, Belmont, California, third edition, 1989.

[11] L. D. Harmon. Automated tactile sensing. *International Journal of Robotics Research*, 1(2):3–31, 1982.

[12] P. Harriott. *Process Control.* McGraw-Hill, New York, 1964.

[13] H. Hemami and R. E. Goddard. Recognition of geometrical shape by a robotic probe. *Journal of Robotic Systems*, 4(2):237–257, 1987.

[14] S. J. Lederman and R. A. Browse. The physiology and psychophysics of touch. In P. Dario, editor, *Sensors and Sensory Systems for Advanced Robots*, volume 43 of *NATO ASI Series F: Computer and Systems Sciences.* Springer-Verlag, Berlin, Heidelberg, 1988.

[15] H. R. Nicholls and M. H. Le. A survey of robot tactile sensing technology. *International Journal of Robotics Research*, 8(3):3–30, 1989.

[16] K. Ogata. *System Dynamics.* Prentice Hall, New Jersey, 1978.

[17] R. C. Oldenbourg and H. Sartorius. The dynamics of automatic controls. *The American Society of Mechanical Engineers*, 77:276, 1948.

[18] Meyer J. R., G. D. Whitehouse, C. L. Smith, and P. W. Murrill. Simplifying process response approximation. *Instruments and Control Systems*, 40(12):76–79, December 1967.

[19] M. H. Raibert. An all digital vlsi tactile array sensor. In *Proc. of the IEEE Int. Conf. on Robotics*, pages 314–319, Washington, D.C., 1984. IEEE Computer Society Press.

[20] S. R. Ruocco. *Robot Sensors and Transducers.* Halsted Press, John Wiley and Sons, New York, 1987.

[21] R. A. Russel. Using tactile whiskers to measure surface contours. In *Proc. of the IEEE Int. Conf. on Robotics and Automation*, pages 1295–1299, 1992.

[22] R. A. Russell. *Robot Tactile Sensing.* Prentice Hall, Sydney, 1990.

[23] J. K. Salisbury, Jr. Interpretation of contact geometries from force measurements. In M. Brady and R. Paul, editors, *Proc. of the First Int. Symposium on Robotics Research*, pages 565–577. M.I.T Press, 1984.

[24] D. E. Seborg, T. F. Edgar, and D. A. Mellichamp. *Process Dynamics and Control.* John Wiley and Sons, New York, 1989.

[25] C. L. Smith. *Digital Computer Process Control.* Intext, Scranton, PA, 1972.

[26] C. L. Smith and P. W. Murrill. A more precise method for tuning controllers. *ISA Journal*, 13(5):50–58, May 1966.

[27] S. A. Stansfield. Primitives, features, and exploratory procedures: Building a robot tactile perception system. In *Proc. of the IEEE Int. Conf. on Robotics and Automation*, pages 1274–1279, 1986.

[28] S. S. Stevens. On the psychophysical law. *Psychological Review*, 64:153–181, 1957.

[29] S. S. Stevens. The surprising simplicity of sensory metrics. *American Psychologist*, 17:29–39, 1962.

[30] R. Tubiana. Architectures and functions of the hand. In R. Tubiana, editor, *The Hand*, volume 1. W. B. Saunders Company, Philadelphia, 1981.

[31] J. V. Vegte. *Feedback Control Systems.* Prentice Hall, New Jersey, 1986.

[32] A. Witkins. Scale space filtering: A new approach to multi-scale description. In S. Ullman and W. Richards, editors, *Image Understanding 1984*. Ablex Publishing Corporation, Norwood, New Jersey, 1984.